ABSTRACT

Title of Document: PROGRAMMED RIBOSOMAL FRAMESHIFTING IN SARS-CoV AND HIV-1

Jessica Joy Neeriemer,
Master of Science, 2007

Directed By: Dr. Jonathan D. Dinman
Cell Biology and Molecular Genetics
University of Maryland

Programmed ribosomal frameshifting controls the ratio of two protein products made in a variety of viruses and mammalian cells. This occurs when the ribosome is translating mRNA, pauses at secondary structure, slips back one base in the 5' direction, and continues translation in a new reading frame. A series of SARS-CoV pseudoknot mutants were generated to examine important features of frameshifting, and an antibiotic was tested for its effect on HIV and SARS-CoV frameshifting. Other mutants were made in the human CCR5 gene to determine whether frameshifting occurs. It was found that mRNA stability and unpaired adenosines influence frameshifting, and increasing concentrations of the antibiotic gentamicin increases frameshifting. Moreover, CCR5, the co-receptor for HIV, contains a working frameshifting signal. This study pinpoints several antiviral targets and important factors for HIV and SARS-CoV pathogenesis.

PROGRAMMED RIBOSOMAL FRAMESHIFTING IN SARS-CoV AND HIV-1

By

Jessica Joy Neeriemer

Thesis submitted to the Faculty of the Graduate School of the
University of Maryland, College Park, in partial fulfillment
of the requirements for the degree of
Master of Science
2007

Advisory Committee:
Dr. Jonathan D. Dinman, Chair
Dr. Jeff DeStefano
Dr. Brenda Fredericksen

Dedication

For my husband, Josh, our daughter Niva, and our wonderful family.

Thank you so much for all your love and support.
I am blessed to have you in my life.

Acknowledgements

There are so many people who have helped me with this project. First, I'd like to thank my mentor, Dr. Jon Dinman. His support, encouragement, and humor have made this possible. His door was always open for questions or discussions.

I also want to thank everyone in the Dinman lab. Without them, I would have lost my sanity, my sense of humor, and half my intelligence. We always seem to have fun and find something to laugh about. I have learned so much because of their willingness to teach.

Jen- What would I have done without you? I'm going to miss our random conversations, your practical tips, and all of our lunch dates. Now we can look forward to the next phase of our life—motherhood!

Michael- You have been a friend throughout grad school. Thanks for suffering with me through many terrible classes. Stay away from sharks and have fun with that soup.

Trey- "Tell me a story!" You always have a good story on hand, and are immensely fun to talk to. Thank you for including me in experiments and trips to the Hippie-mart.

Rasa- The "Queen" of the lab! I have yet to find a question you can't answer.

Arturas- Your smile and knowledge light up the lab.

A huge thanks and hugs to Josh and our family for their constant encouragement. You were always there to celebrate my successes and pick me up when I was discouraged. Your faith in me never wavered.

Table of Contents

List of Tables

List of Figures

Chapter 1: Introduction- Ribosome Structure and Function

The process of translating messenger RNA (mRNA) to protein is fundamental in the cell, but it certainly isn't simple. After genes are transcribed into mRNAs, the ribosome is responsible for converting the information contained in nucleotide sequences to amino acids to form proteins. Ribosomes are thus essential to all forms of life. The ribosome is a complex machine made up of RNA and protein. It consists of approximately 30% protein and 70 % RNA. The ribosome is made up of two different subunits that are required to work together to translate mRNAs.

Despite the fact that ribosomes are highly conserved, there are differences between the kingdoms. In bacteria, the subunits are called the 30S subunit, or the small subunit, and the 50S subunit, or the large subunit. When joined, they form a 70S complex. In eukaryotes, the subunits are 40S (also known as the small subunit) and 60S (or large subunit), and come together to form an 80S complex. The RNA component in bacteria is made up of three species named 5S, 16S, and 23S. The large subunit contains the 5S and 23S rRNA and 33 proteins, while the small subunit is made up of the 16S rRNA and 21 proteins (Wilson & Nierhaus, 2003; Nilsson *et al*, 2007). In eukaryotic ribosomes, the large subunit contains 45 proteins, 25S rRNA, 5S rRNA, and 5.8S rRNA (Nilsson *et al,* 2007). The small subunit is made up of 33 ribosomal proteins and 18S rRNA.

Overall, eukaryotic ribosomes are about 30% larger than prokaryotic ribosomes (Wilson & Nierhaus, 2003). The differences lie in expansion segments of

rRNA, meaning that they contain additional sequence, and additional ribosomal proteins. Because of the conservation of functional centers, the differences are located mostly along the periphery of the ribosome.

The ribosome's functional centers include three tRNA binding sites, known as the A, P, and E sites, decoding center, and peptidyltransferase center. These are all used throughout the steps of initiation, elongation, and termination, where each cycle adds a new amino acid. Approximately ten to twenty amino acids are added per second in the cell (Wilson & Nierhaus, 2003). As translation is responsible for making functional proteins, it is important to accurately decode the mRNA into protein. The error rate of translation in vivo is estimated to between 10^{-3} and 10^{-4} (Ogle *et al,* 2005), which corresponds to one error in about 3000 codons (Wilson & Nierhaus, 2003). These errors are typically due to incorrect aminoacylation of tRNA, incorrect tRNA selection by the ribosome, or incorrect maintenance of the reading frame (Ogle *et al*, 2005).

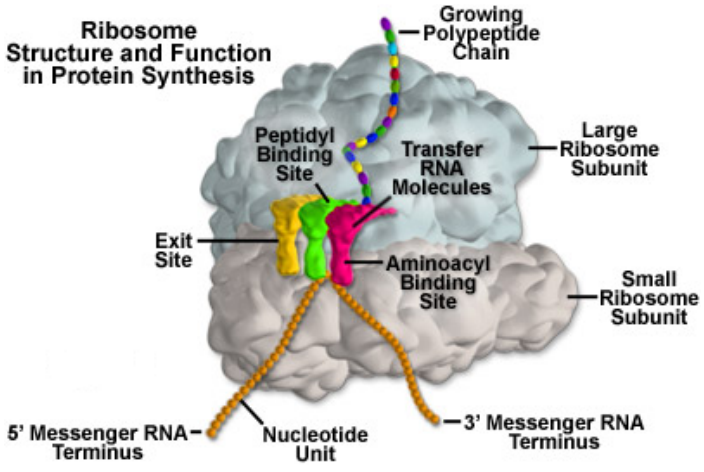

Figure 1. *Representation of the ribosome*. The large and small subunit come together to carry out translation. Bound tRNAs are depicted in the diagram, as well as the mRNA and peptide channels. The peptidyl transferase center would be located directly above the A and P sites, while the decoding center is found on the small

subunit under the A site.
(http://micro.magnet.fsu.edu/cells/ribosomes/images/ribosomesfigure1.jpg)

For initiation to begin, the ribosome must exist as separate subunits (Demeshkina *et al*, 2007). During resting phase or under stressful conditions, ribosomes are joined into 70S or 80S particles. Bacteria use elongation factor G and ribosome recycling factor to catalyze the dissociation of free 70S ribosomes. This is powered by GTP hydrolysis, although the dissociation is transient (Demeshkina *et al,* 2007). IF3 is required to keep the subunits apart by binding to 30S subunits. IF3 is sufficient to split the 70S ribosomes, but is slow by itself. In eukaryotes, several eukaryotic initiation factors have activity similar to IF3, e.g. eIF1A, eIF1, and eIF3. eIF6 also has strong dissociation activity on 80S ribosomes. However, active dissociation of ribosomes is thought to be carried out by eEF2 in a process that requires ATP hydrolysis and is hindered by GTP (Demeshkina *et al,* 2007). The reaction is also transient and requires further stabilization by ribosome anti-association factor or by treating the reaction with glutaraldehyde (Demeshkina *et al,* 2007).

To begin initiation in bacteria, the mRNA has to bind the 30S subunit. The Shine-Delgarno sequence is complementary to the 3' end of 16S rRNA and binding places the ribosome at the appropriate spot on the mRNA (Uemura *et al,* 2007; Ogle *et al,* 2005). Initiation factors IF1, IF2, and IF3 are all required for initiation. The initiator tRNA, Met-$tRNA_i^{Met}$, is bound to the P site. This initial binding is promoted by IF2 and stabilized by IF3 (Gualerzi *et al*, 1977). The interactions between the Shine-Delgarno sequence and the ribosome also help stabilize the entire complex on the mRNA. There is a conformational change, and IF1 and IF3 are ejected from the

complex. IF2 then promotes binding of the 50S subunit (Laursen *et al*, 2005). However, after the first peptide bond is formed these interactions are relaxed, which allows for translocation of the ribosome (Uemura *et al,* 2007).

Eukaryotic initiation is much more complicated. eIF1, eIF1A, eIF3, and eIF5 combine to form the multifactor complex (Fekete *et al*, 2007). All of these factors are required to recruit the 43S pre-initiation complex, which includes the initiator tRNA, Met-$tRNA_i^{Met}$, as a ternary complex with GTP and eIF2 bound to the 40S subunit. The entire complex binds to the mRNA and then scans to find the first AUG in a good context. The scanning process is stimulated directly by eIF1 and eIF1A. Their binding causes an open conformation in the small subunit that moves the head and platform of the 40S, and results in increasing accessibility of the mRNA channel (Gilbert *et al,* 2007). That allows for the scanning movement and restricts base pairing of non-AUGs with Met-$tRNA_i^{Met}$ (Fekete *et al,* 2007). Once the AUG start codon binds the Met-$tRNA_i^{Met}$ in the P site, eIF1 and eIF1A move apart from each other and eIF1 is released. This causes GTP hydrolysis and thus accommodation of the initiator tRNA. The resulting conformational changes and interaction with eIF5 causes eIF1A to bind more tightly and restricts the mRNA channel so that scanning stops (Fekete *et al,* 2007).

After the initiator tRNA is bound and the 60S subunit has joined, the ribosome must decode the next codon of the mRNA. This process is broken up into two steps, decoding and accommodation. During decoding, the next aminoacyl-tRNA is brought to the ribosome as a ternary complex with GTP and EF-Tu in bacteria or eIF1A in eukaryotes. At this point the A site is in a low affinity state where interactions are

reduced with the ternary complex (Wilson & Nierhaus, 2003). Only the codon and anticodon interact with a small amount of discrimination energy.

The codon:anticodon interaction is monitored spatially by 16S rRNA bases in the A site. These bases include G529, G530, A1492, and A1493, which are all required for viability and tRNA binding (Ogle *et al*, 2005). When a cognate tRNA is in the A site, A1492 and A1493 are displaced into the minor groove of helix 44, and G530 switches from a *syn* to *anti* conformation. The first base pair between the codon and anticodon is monitored through a type I A-minor motif, while the second base pair is monitored by a type II A-minor motif (Wilson & Nierhaus, 2003; Ogle *et al,* 2005). The second base pair is stricter than the first, but the third is not highly monitored. Hence the wobble position in codons. These interactions induce a conformational change that results in a global domain closure of the 30S shoulder (Ogle *et al*, 2005).

If there is incorrect binding, meaning the aa-tRNA is near-cognate or noncognate, these conformational changes do not occur and the aa-tRNA will diffuse out of the A site (Taliaferro & Farabaugh, 2007). The difference in binding rate constants are 100-fold, where the preference for cognate tRNAs are 10,000-fold greater. Also, the observed accuracy rates are due to the rate of activation of the GTPase and elongation factor (Taliaferro & Farabaugh, 2007).

This leads to the next step of accommodation. The domain closure leads to GTP hydrolysis, which provides the energy needed to relax the constrained anticodon stem loop of the distorted aa-tRNA, and release of EF-Tu. This allows the acceptor arm of the tRNA to "pop" into the peptidyltransferase center in the large subunit.

That means there has to be communication between the decoding center in the small subunit to the binding site of the ternary complex. This occurs through the tRNA body and intersubunit bridges (Cochella *et al,* 2007). Accommodation, then, is the rate-limiting step of aa-tRNA selection (Wilson & Nierhaus, 2003).

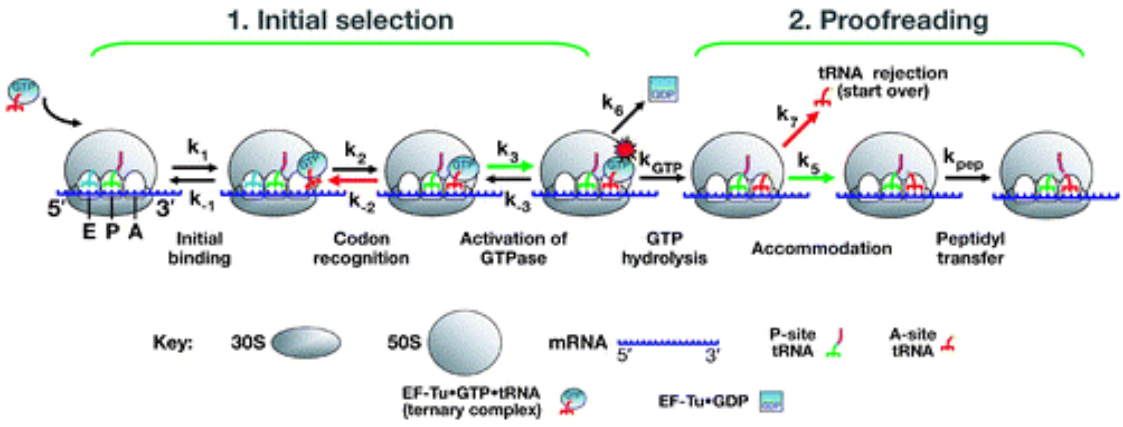

Figure 2. *A schematic representation of tRNA selection during elongation on the ribosome.* The first step shows decoding, while the second depicts accommodation. Red arrows show rates that are higher for near-cognate tRNA, whereas green ones show those that are higher for cognate tRNA (Ogle & Ramakrishnan, 2005).

Immediately after accommodation, peptidyl transfer occurs. This requires the ribosome to have tRNAs in both the A and P site. The peptidyltransferase center (PTC) is located in the large subunit of the ribosome. The PTC is the catalytic site for transferring the nascent peptide chain from the peptidyl-tRNA in the P site to the aminoacyl-tRNA in the A site, thus growing the peptide chain by one amino acid. The catalytic center is made exclusively by rRNA and the mechanism is universally conserved (Wilson *et al*, 2005). There are no proteins within 15 Å of the active site, but ribosomal proteins are important for providing a framework and organizing the PTC. (Bieling *et al*, 2006; Polacek & Mankin, 2005).

The PTC is located at the bottom of the large cleft on the interface side of the large subunit underneath the central protuberance (Polacek & Mankin, 2005; Rodnina *et al*, 2006). The acceptor ends of the tRNAs meet at the bottom of the funnel-shaped active site above the entrance to the peptide exit tunnel, and are stabilized by the 23S rRNA (Polacek & Mankin, 2005). The P-tRNA bases C74 and C75 base pair with G2252 and G2251 of the 23S rRNA P-loop. The A-tRNA is fixed in position by pairing C75 with G2553 of the A-loop. Moreover, there are A-minor interactions between A76 and base pairs G2252-G2251 and A2450-C2501 (Rodnina *et al*, 2006). The flexibility of the ribosome allows an induced-fit mechanism to promote tight binding and orientation of the tRNAs (Davidovich *et al*, 2007).

The peptidyl transfer reaction consists of the α-amino group of the A-tRNA attacking the carbonyl group of the peptidyl residue of the P-tRNA. Thus the P-tRNA becomes deacylated and the A-tRNA gains the peptide (Wilson *et al*, 2005; Bieling *et al*, 2006; Polacek & Mankin, 2005). There are several possible ways to catalyze this reaction: abstraction or donation of protons, orientation and proximity effects, removing water from the active site, stabilizing the transition state by electrostatic interactions, and having a preorganized electrostatic environment which decreases the activation energy of the transition state (Bieling *et al*, 2006).

There has been much debate as to whether transpeptidation happens through an acid-base mechanism. Through many biochemical and mutational studies, it has been concluded this is not the case (Rodnina *et al*, 2006; Beringer & Rodnina, 2007). Currently the favorite model proposes that the ribosome catalyzes transpeptidation by reducing the entropy of the reaction by locking the tRNAs in the proper orientation,

desolvation, and electrostatic shielding (Polacek & Mankin, 2005; Rodnina *et al*, 2006). Peptidyl transfer occurs as a rate of 15-50 peptide bonds per second, which is a $4x10^6$ –fold acceleration compared to the uncatalyzed reaction (Bieling *et al*, 2006, Beringer & Rodnina, 2007).

After peptidyl transfer, there is a deacylated tRNA in the P site and a peptidyl-tRNA in the A site. To continue the elongation cycle, translocation must occur to move the deacylated tRNA into the E site and the peptidyl-tRNA into the P site. All the interactions between the tRNAs, mRNA, and the ribosome, as well as intersubunit bridges, must be broken and then reestablished, while maintaining the correct reading frame. Movement from one site to another is a distance of 30Å (Munro *et al*, 2007).

Translocation is a complicated and dynamic process. First the translation factor EF-G in bacteria or eEF2 in eukaryotes binds to the ribosome after peptidyl transfer. This stabilizes the tRNAs in the so-called hybrid state, where the tRNA acceptor arms are in the next functional site in the large subunit while the anticodon stem loops remain in the classical position (Rodnina *et al*, 1999). For example, the A-tRNA would move from the classical A/A state to the A/P hybrid state, with the acceptor arm in the P site and the anticodon in the A site (Pan *et al*, 2007; Li & Frank, 2007). The P-tRNA moves from the P/P state to the P/E hybrid state. Binding of EF-G/eEF2 also induces conformational rearrangements in the ribosome such that there is a ratcheting motion of the small subunit relative to the large subunit. This moves the anticodon stem loops of the tRNAs 8Å toward the next functional site (Taylor *et al*, 2007). Movement of the tRNAs enable domain IV of EF-G/eEF2 to reach into the A site and prevent backwards movement (Ortiz *et al*, 2006). GTP is hydrolyzed and

induces further conformational rearrangement, which leads to another 6Å shift of domain IV (Rodnina *et al*, 1999; Ortiz *et al*, 2006; Horan *et al*, 2007). The codon:anticodon interaction is thus broken, and allows the head of the small subunit to rotate. This moves the tRNAs the rest of the way into the respective E and P sites. EF-G/eEF2 then dissociates from the ribosome, which shifts back to its pre-translocation state (Taylor *et al*, 2007).

Despite all the complicated steps, translocation is a fast process that is not rate-limiting to the elongation cycle. This is because GTP hydrolysis lowers the activation energy, but is not required to drive the reaction thermodynamically (Rodnina *et al*, 1999; Taylor *et al*, 2007).

Translocation results in binding a deacylated tRNA in the E site. Peptidyl-tRNA or aminoacylated-tRNA cannot bind the E site (Wilson & Nierhaus, 2003). There are many interactions that hold the tRNA in place. In the small subunit, the rRNA joins with the ASL via backbone-backbone interactions, as well as the C-terminal α helix of S7 (in bacteria) (Korostelev *et al*, 2006; Selmer *et al*, 2006). In the large subunit, the acceptor end of the tRNA makes backbone-backbone interactions with Helix 68, and touches ribosomal proteins L1 and L28 (Korostelev *et al*, 2006). The tRNA is further stabilized by base stacking (Selmer *et al*, 2006).

The E site stands for "exit" site. There cannot be more than two tRNAs on an active ribosome at one time so to continue the elongation cycle, the deacylated tRNA in the E site needs to be released (Wilson & Nierhaus, 2003; Dinos *et al*, 2005). This requires another translation factor in yeast, eEF3. eEF3 is specific to yeast, has ATPase activity, interacts with both subunits, competes with eEF2 for binding, and

stimulates eEF1A-dependent binding of aa-tRNAs (Andersen *et al*, 2006). eEF3 has two domains that span the central protuberance of the large subunit and the head of 40S. It binds specifically to the post-translocation state of the ribosome, simultaneously with eEF1A. Upon binding the ribosome, there is a conformational change that results in ATP hydrolysis and the dissociation of eEF3. The conformational change also relaxes the interactions that hold the E-tRNA in place, and that deacylated tRNA is released from the ribosome. This occurs when the aa-tRNA has been decoded, but before GTP hydrolysis and accommodation (Dinos *et al*, 2005).

As eEF3 is a specific elongation factor in yeast, it has been shown that in other eukaryotes and bacteria the E-tRNA is released upon movement of the L1 stalk due to conformational rearrangement of the ribosome when the ternary complex binds (Wilson & Nierhaus, 2006). There is no elongation factor necessary.

The final step in translation is termination, or nascent peptide release. When a stop codon on the mRNA is in the A site, release factors bind the ribosome. The tip of domain III of the release factor reaches into the peptidyl transferase center to promote hydrolysis of the peptidyl-tRNA ester bond (Polacek & Mankin, 2005). There is an activated water molecule that undergoes a nucleophilic attack on the carbonyl of the 3' terminal adenosine of the P-tRNA (Amort *et al*, 2007). This releases the peptide from the tRNA, and can thus exit the ribosome. If the reaction was uncatalyzed, termination would occur once in 14 hours (Polacek & Mankin, 2005). However, like peptidyl transfer, the reaction is entirely catalyzed by rRNA and thus the reaction

occurs approximately once per second (Polacek & Mankin, 2005; Beringer & Rodnina, 2007).

The PTC, then, has a dual role to play during translation. It has to perform catalysis of both transpeptidation and peptide release. Studies have shown that the 23S rRNA base A2602 is important in both reactions. A2602 is a flexible base that is central in the PTC. It was hypothesized that A2602 coordinates and activates the water molecule that is responsible for the nucleophilic attack during termination only (Polacek & Mankin, 2005; Amort *et al*, 2007). However, there is a new model that predicts that the ribosome release factor in the A site orients A2602, and can act as a molecular switch. During termination, A2602 is pulled out of the center of the PTC to guide a water molecule into the active site (Amort *et al*, 2007). The 2' hydroxyl of A76, then, could be responsible for coordinating and activating that water molecule.

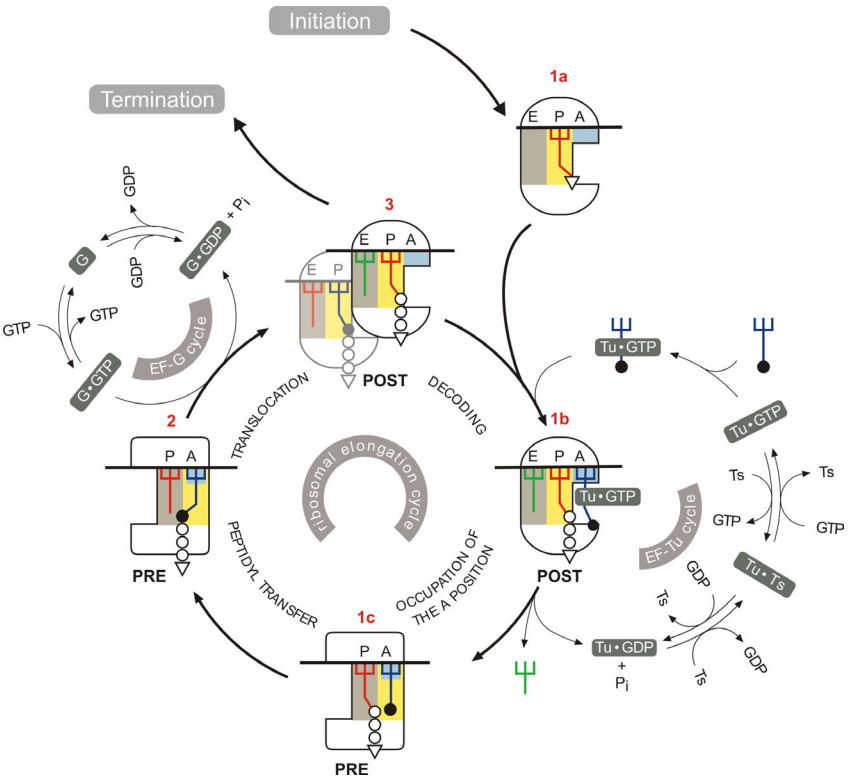

Figure 3. Summary of elongation cycle during bacterial translation using the allosteric three- site model.

Elongation occurs through the steps of decoding and accommodation, peptidyl transfer, and translocation (Dinos *et al*, 2005).

Chapter 2: Introduction- Programmed Ribosomal Frameshifting in SARS-CoV and HIV

Programmed ribosomal frameshifting (PRF) is a mechanism that allows translation of a downstream open reading frame. This process is used by many RNA viruses, as a method to minimize genome space and to regulate the stoichiometry of protein products. Viruses are obligated to condense their genomes as much as possible due to space constraints in packaging the genome and time constraints during replication. It has been shown that many (+)ssRNA viruses, dsRNA viruses, plant viruses, and bacteriophages all utilize the frameshifting mechanism (Brierley & Dos Ramos, 2005).

In viruses, the frameshift signal is typically located between the structural genes and the enzymatic genes. The most common example is the *gag* gene, which encodes the protein necessary to build the capsid structure that packages the genome, and the *pol* gene, which encodes the polymerase that replicates the viral genome (Jacks *et al*, 1988; Dinman *et al*, 2002; Brierley & Dos Ramos, 2005). The ribosome will translate the *gag* gene, and the majority of the time it will terminate at the *gag* 0-frame stop codon. A certain proportion of the time, however, the ribosome will frameshift and slip into a new open reading frame. This allows the *pol* gene to be translated as a fusion peptide with the *gag* gene. The efficiency of the frameshift determines the ratio between the structural and enzymatic proteins.

If the frameshifting efficiency is changed, it can have dramatic effects on viral propagation (Dinman & Wickner, 1992; Léger *et al*, 2007). This was first shown with

the L-A virus, a dsRNA virus that infects yeast. There is a programmed ribosomal frameshift signal between the *gag* and *pol* genes. The L-A virus supports a satellite virus called M_1, which encodes a toxin that kills surrounding yeast and thus confers a selective advantage to the host. The wildtype frameshifting efficiency is 1.9% so there are approximately 2 gag-pol fusion peptides per virion (Dinman & Wickner, 1992). If the efficiency of frameshifting is changed, L-A cannot maintain M_1, demonstrating that viral fitness is decreased.

This is also true for HIV-1. Similar to L-A, there is a frameshift signal between the *gag* and *pol* genes. Typical frameshifting efficiency is about 2 to 10% of the time, depending on what system is used to measure it (Jacks *et al*, 1988). When mutations were made in the slippery site or the stimulatory structure, frameshifting decreased (Jacks *et al*, 1988; Dulude *et al,* 2005; Plant & Dinman, 2006). Correspondingly, there was a decrease in activity of the polymerase and a decrease in infectivity (Dulude *et al,* 2005). This shows a direct correlation between frameshift efficiency and viral propagation. Thus frameshifting can be used as an antiviral target.

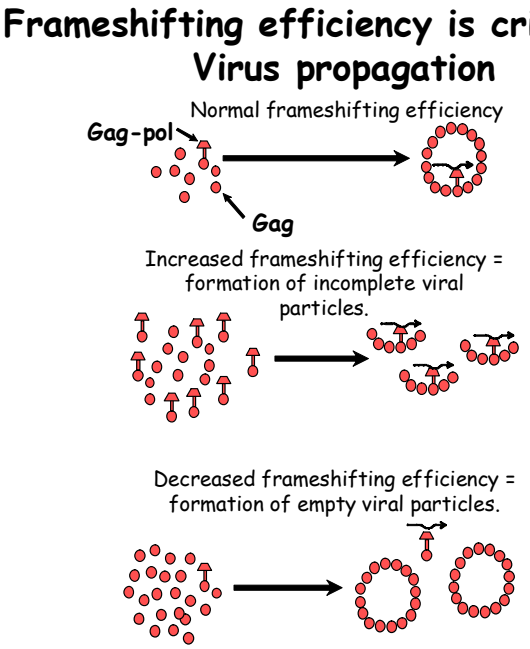

Figure 4. *Importance of frameshifting efficiency on viral propagation in terms of viral assembly.* Increasing the amount of frameshifting leads to incomplete or unformed viral particles, whereas decreased frameshifting leads to empty viral particles. Both results in a decrease in viral infectivity.

Frameshifting has been found in retrotransposons and mammalian genes as well. In many neurodegenerative diseases insoluble protein aggregates are found. Examples of these proteins are ubiquitin B and β-amyloid precursor protein (Wills & Atkins, 2006). The aberrant forms of these proteins contain C-termini that are encoded by alternate reading frames. These proteins have been implicated in such diseases as Alzheimer's, Huntington's, and spinocerebellar ataxias, and it is hypothesized that the aberrant form is caused by frameshifting (Wills & Atkins, 2006).

A programmed -1 ribosomal frameshift signal consists of three basic features: a heptameric slippery site, a spacer region of 6-9 nucleotides, and a downstream stimulatory structure. As the ribosome is translating, it pauses when it encounters the mRNA secondary structure (Takyar *et al*, 2005). The spacer region positions the

ribosome over the slippery site during the pause. The slippery site motif is X XXY YYZ, where the spacing indicates the incoming reading frame. X can be any three identical nucleotides, Y can be AAA or UUU, and Z can be any nucleotide but G (Plant et al, 2003; Hansen *et al*, 2007; Léger *et al*, 2007). The stimulatory structure is typically a pseudoknot, although it has been shown that some stem loops can induce frameshifting.

Pseudoknots are a type of RNA secondary structure. These are formed when downstream sequence base pairs with the loop of a hairpin, although there are many variations on this theme (Puglisi *et al*, 1988). Pseudoknots have structural and functional roles, including the G-ribo motif pseudoknots in the ribosome (Steinberg & Boutorine, 2007). The stability of the pseudoknot is important for frameshifting efficiency: the more stable it is, the longer the ribosome pauses (Tu *et al*, 1992; Namy *et al*, 2006). However, there is no correlation between absolute frameshifting percentage and ΔG free energy (Giedroc *et al*, 2000; Hansen *et al*, 2007).

There are many different models as to how frameshifting occurs. The first proposes that the stimulatory structure acts as a binding site for a protein factor that is responsible for frameshifting (Brierley & Dos Ramos, 2005). However, no protein factor has ever been found, although this model can't be ruled out. The second model suggests that the ribosome pauses at the stimulatory structure, which gives sufficient amount of time for the slip to occur (Tu *et al*, 1992). The emphasis on the importance of the RNA secondary structure is appropriate, but is not the sole determining factor (Namy *et al*, 2006). The third model is the simultaneous slippage model, where both

tRNAs bound to the A and P site re-base pair in the -1 frame (Jacks *et al*, 1988; Léger *et al*, 2007).

Within the simultaneous slippage model, there is debate as to when the frameshifting event happens during the elongation cycle. One argument is called the 9 Å model. The pseudoknot interacts with the ribosome at the entrance to the mRNA channel. The ribosome has helicase activity located between the head and shoulder of the small subunit, and tries to unwind the pseudoknot (Jacks *et al*, 1988; Takyar *et al*, 2005; Namy *et al*, 2006). This induces supercoiling and puts tension on the mRNA (Plant *et al*, 2003; Hansen *et al*, 2007). The model includes an occupied P site with an aminoacyl-tRNA that is being decoded in the A site, and exists in the hybrid A/T state. There is a 9 Å movement of the anticodon stem loop of the aa-tRNA during accommodation, but this movement is restricted by the tension on the mRNA due to being unable to unwind the pseudoknot and its blockage of the mRNA entrance tunnel (Plant *et al*, 2003; Namy *et al*, 2006; Hansen *et al*, 2007). The tension is relieved by having the tRNAs re-base pair in the -1 frame. This model, then, says that frameshifting occurs with a P-tRNA and an aa-tRNA that is not yet accommodated. Thus, it occurs before peptidyl transfer.

Another proposal is that frameshifting occurs during translocation. The elongation factor is bound to the ribosome and prevents binding to the A site until translocation and frameshifting occurs (Namy *et al*, 2006). The pseudoknot blocks the mRNA entrance channel and prevents accurate eEF2-catalyzed translocation (Plant *et al*, 2003). Instead of being able to shift the mRNA a complete codon, the mRNA is only moved two nucleotides. The added tension in the mRNA caused by the

stimulatory structure pulls on the P-tRNA towards the A site and raises the anticodon. Since the P-tRNA can't return to the A site and translocation was incomplete, the strain on the tRNAs cause breakage and rebinding of the codon:anticodon in the -1 direction (Namy *et al*, 2006). One of the attractive points of this model is that fact that GTP hydrolysis supplies the energy for the breaking and reforming of the hydrogen bonds between the tRNAs and mRNA (Plant *et al*, 2003).

The other arugment proposes that frameshifting happens before translocation. tRNAs that are in the hybrid state can unpair from the mRNA, move one base in the upstream 5' direction, and re-pair. The anticodon stem loops can then move with the mRNA to the P and E sites (Léger *et al*, 2007).

The above two models have been integrated to propose that frameshifting is triggered by incomplete translocation, and happens, then, after peptidyl transfer. The tRNAs are in the hybrid state, where acceptor stems are in an intermediate position between the PRE and POST states of the translocated ribosome. The anticodon stem loops move to the classical E/E and P/P sites, which drag the mRNA by 1 codon. However, some mRNAs can only drag the mRNA by 2 bases due to the constraint of being unable to unwind the RNA secondary structure downstream. Thus, the tRNAs are block in intermediate sites, and the incoming aa-tRNA is blocked as well. Therefore, the interactions between the codons and anticodons break and re-form, starting in the E site. This causes an overall change in the reading frame in the -1 direction (Léger *et al*, 2007).

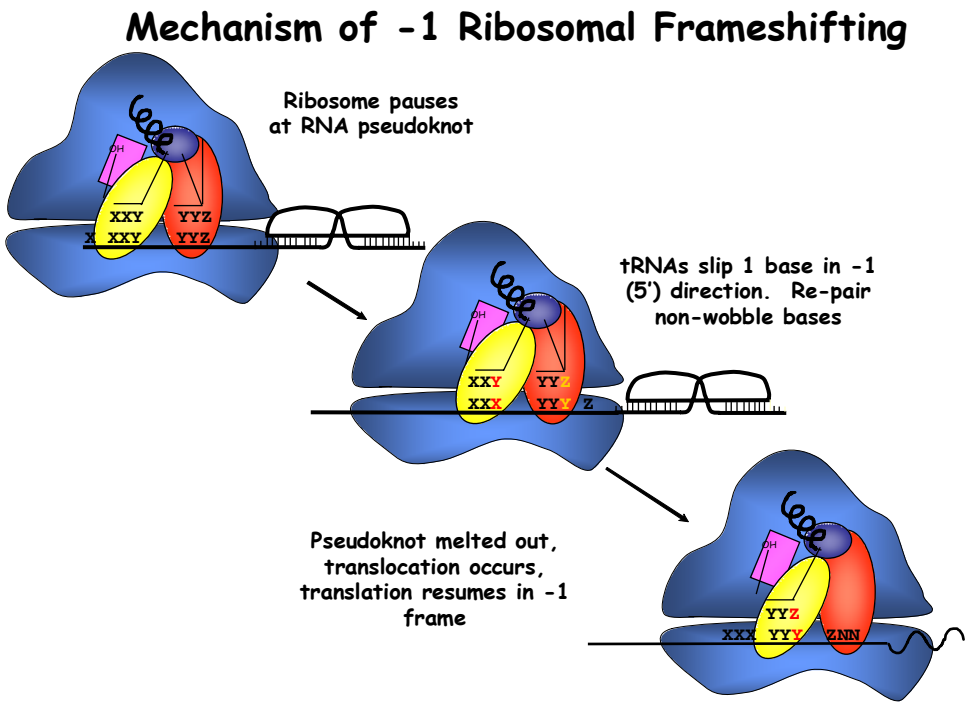

Figure 5. *Mechanism of -1 Programmed Ribosomal Frameshifting.* As the ribosome translates certain mRNAs, it pauses when it encounters a stable secondary structure, typically a pseudoknot. The bound tRNAs uncouple from the mRNA and repair in the -1 frame. Then the pseudoknot is unwound and translation continues in the -1 open reading frame.

It is important to point out that these models for ribosomal frameshifting do not have to be mutually exclusive.

Regardless of when frameshifting occurs during translation, other factors are important for determining if frameshifting occurs and its efficiency. The sequence of the slippery site can have a profound impact (Plant & Dinman, 2006; Hansen *et al*, 2007). Some slippery sites are more "slippery" than others, particularly homopolymeric sequences and those without Gs or Cs (Brierley & Dos Ramos, 2005; Namy *et al*, 2006). These are nucleotides that have more hydrogen bonds and thus require more energy to break the codon:anticodon interactions. The nucleotide

sequence surrounding the slippery site can also influence frameshifting (Brierley & Dos Ramos, 2005; Hansen *et al*, 2007).

As previously mentioned, the stability of the pseudoknot impacts the frameshifting efficiency. The less stable a pseudoknot or secondary structure is, the less frameshifting occurs. The ability of the pseudoknot to resist unwinding by the ribosome and the energy barriers to unfolding the pseudoknot are both factors of efficiency (Plant & Dinman, 2005). Modifications to the tRNAs in the A and P site can affect the stability of the codon:anticodon interactions and change the frameshifting efficiency (Plant & Dinman, 2006). Also, mutations in the E site or rRNA in the platform of the small subunit can affect frameshifting (Léger *et al*, 2007). In general, structural changes to the ribosome can have a profound impact.

Human Immunodeficiency Virus (HIV) is the etiological agent of AIDS. It is a (+)ssRNA virus that is a member of the Retroviridae family. There are two copies of its 9kb genome packaged together into virions through a kissing loop interaction. The helical nucleocapsid also contains 50-100 copies each of reverse transcriptase, integrase, and protease. HIV infects certain immune cells by binding to the CD4 and CCR5 receptors through its envelope protein gp120 (or SU/TM). Fusion of the viral envelope with the cell membrance allows the viral capsid to enter the cytoplasm, where it undergoes reverse transcription. The enzyme reverse transcriptase converts the RNA genome into cDNA, which is transported into the nucleus and integrated into the host genome. The viral proteins are produced through host transcription and translation, similarly to new genomes being made through transcription. Virions are

assembled at the cell membrane, where they exit by budding. Maturation occurs after budding and produces infectious virus.

The viral structural protein that is responsible for forming the capsid is called Gag, and is located on the 5' end of the genome. Gag overlaps with the *pol* gene, which encodes the reverse transcriptase, protease, and integrase (Jacks *et al*, 1988; Dinman *et al*, 2002). Hence, to translate the downstream *pol* gene, there must be a frameshift.

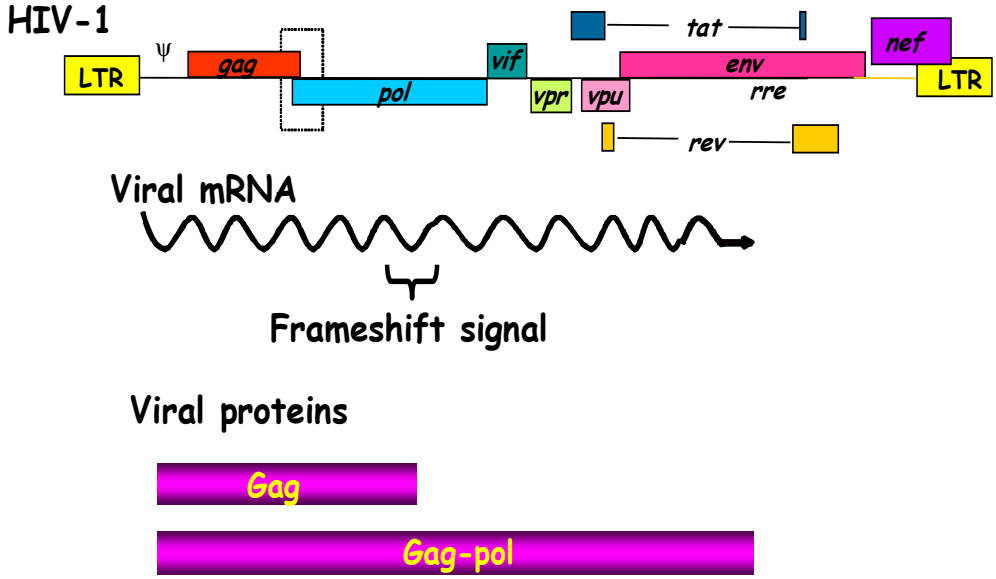

Figure 6. *Genomic organization of HIV*. The *gag* and *pol* genes overlap so there must be a frameshift signal that directs translation of the *pol* gene. The majority of the time just the gag structural protein is made, but when a frameshift occurs the Gag-pol fusion protein is generated.

Studies on the HIV frameshift signal have shown that the frameshift occurs between two and ten percent of the time (Girnary *et al*, 2007). That means there is a Gag to pol ratio between 20:1 and 60:1 (Dinman *et al*, 2002). As previously

mentioned, maintaining the stoichiometry between the structural and enzymatic proteins is crucial for viral propagation. The slippery site is U UUU UUA, where the spacing indicates the incoming reading frame, and is universally conserved among HIV isolates (Dinman *et al*, 2002; Brierley & Dos Ramos, 2005; Girnary *et al*, 2007). Unlike SARS-CoV, the slippery site is located 200 nucleotides upstream of the gag stop codon (Brierley & Dos Ramos, 2005).

The stimulatory structure of the HIV frameshift signal has been highly debated. Many different structures have been proposed to be the cause of frameshifting. It has been shown and accepted that the solution structure of the stimulatory structure is a highly stable stem loop (Stable & Butcher, 2005; Brierley & Dos Ramos, 2005). There is a purine bulge that interrupts the stem loop. It is unusual to have a stem loop stimulate frameshifting and is the exception that the stimulatory structure is a pseudoknot (Dinman *et al*, 2002). However, the slippery site resides at the base of the stem loop so it has been proposed that the ribosome unwinds the lower stem as it translates the mRNA (Léger *et al*, 2007). This would place the slippery site in the A and P sites of the ribosome so the upper stem, then, would act as the stimulatory structure. The 3' half of the lower stem would be free to come back and base pair with the upper stem, forming a triplex (Dinman *et al*, 2002). It has been suggested that there is a conformational equilibrium between the two positions, and the actual structure that promotes frameshifting is the triple helix.

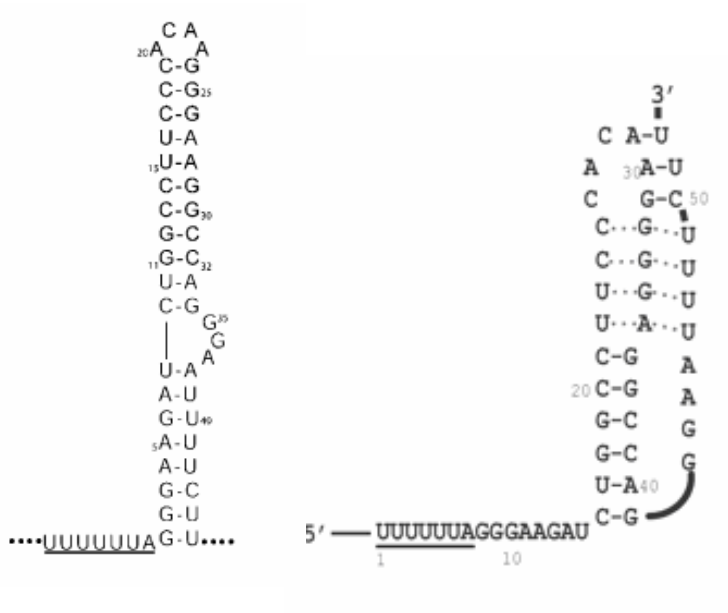

Figure 7. *Solutions of the HIV frameshift stimulatory signal.*

The left stem loop is the solution structure solved by NMR (Stable & Butcher, 2005). The structure on the right is the triplex that could form when the bottom stem is melted by the ribosome (Dinman *et al*, 2002). The slippery site is underlined.

In November 2002, there was an outbreak of a new disease in Guangdong Province of China. By February 2003, it had moved to Hong Kong and further spread to over twenty-five other countries (Thiel *et al*, 2003; Brierley & Dos Ramos, 2005). The disease was called severe acute respiratory syndrome, or SARS. It was marked by fever, dyspnea, lower respiratory tract infection and gastrointenstinal symptoms (Rota *et al*, 2003; Weiss & Navas-Martin, 2005). By July 2003, the outbreak had been controlled through patient isolation and was considered over (Brierley & Dos Ramos, 2005; Weiss & Navas-Martin, 2005). There were over 8,000 cases of SARS worldwide and over 800 deaths.

The global attention on the outbreak spurred international research, and it was announced on March 24, 2003 that SARS was caused by a new human coronavirus, called SARS-CoV (Rota *et al*, 2003). As a member of the coronavirus family, it is a (+)ssRNA virus with a genome of 29.7 kb (Rota *et al*, 2003; Thiel *et al*, 2003;

Brierley & Dos Ramos, 2005). It is an enveloped virus that infects cells by attaching its spike protein to the angiotensin-converting enzyme 2 receptor (Weiss & Navas-Martin, 2005). The binding induces a conformational change that allows fusion of the viral envelope with the host cell membrane, and the nucleocapsid can enter the cytoplasm. Here SARS-CoV can have its genome translated, as its genome can also function as mRNA. Once the RNA-dependent RNA polymerase (RDRP) has been synthesized, replication of the viral genome also begins. It is believed that SARS-CoV assembles at the Golgi intermediate compartment, and the envelope is acquired by budding into vesicles. The vesicles ship the viral particles to the cell surface, where they exit the cell for further infections.

SARS-CoV has a genomic organization where the replicase gene is located at the 5' 22kb (Rota *et al*, 2003; Thiel *et al*, 2003; Weiss & Navas-Martin, 2005). Then the structural genes are encoded: spike, envelope, membrane, and nucleocapsid proteins (Rota *et al*, 2003; Thiel *et al*, 2003; Brierley & Dos Ramos, 2005). The structural proteins are made through subgenomic mRNAs, while the replicase gene is translated in two parts through a frameshift mechanism (Thiel *et al*, 2003).

During typical translation, the 5' end of the replicase gene is translated only, known as orf1a. Approximately 14 to 28% of the time, orf1b is also translated to generate the polyprotein orf1ab (Thiel *et al*, 2003; Brierley & Dos Ramos, 2005; Weiss & Navas-Martin, 2005). Orf1a is processed into eleven proteins by two cysteine proteases (Thiel *et al*, 2003). Orf1b is processed into five proteins, including the RDRP, helicase, exonuclease, endoribonuclease, and a methyltransferase (Thiel *et al*, 2003; Brierley & Dos Ramos, 2005). The frameshift signal was discovered to

contain all the expected features- a slippery site, a spacer region of seven nucleotides, and a downstream pseudoknot (Thiel *et al*, 2003; Su *et al*, 2005). The slippery site of the frameshift signal was determined to be U UUA AAC (Baranov *et al*, 2005; Plant *et al*, 2005; Su *et al*, 2005), and is found twelve nucleotides upstream from the orf1a stop codon.

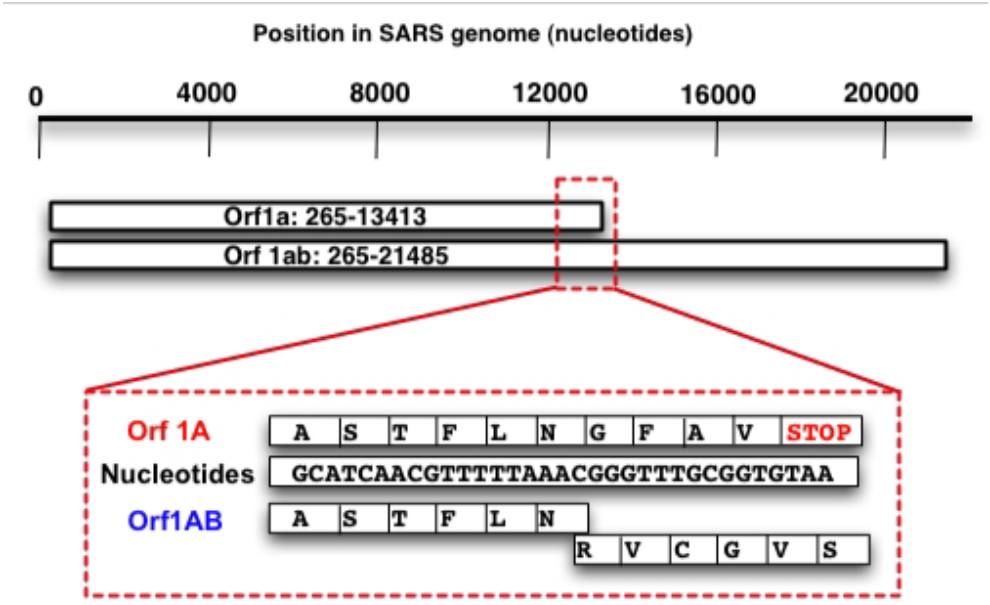

Figure 8. *Organization of SARS-CoV replicase gene.* Orf1ab encodes sixteen proteins that are important for viral replication and pathogenesis, including the RNA-dependent RNA polymerase in orf1b. The orf1ab fusion protein is only made through a ribosomal frameshift, which is located only twelve nucleotides upstream from the orf1a stop codon.

Studies on the SARS-CoV frameshift signal have characterized the pseudoknot as a unique three-stemmed pseudoknot (Plant *et al*, 2005). Early studies initially showed a typical H-type pseudoknot, but computational, molecular, biophysical, and genetic evidence have shown the presence of a third stem-loop (Thiel et al, 2003; Plant *et al*, 2005).

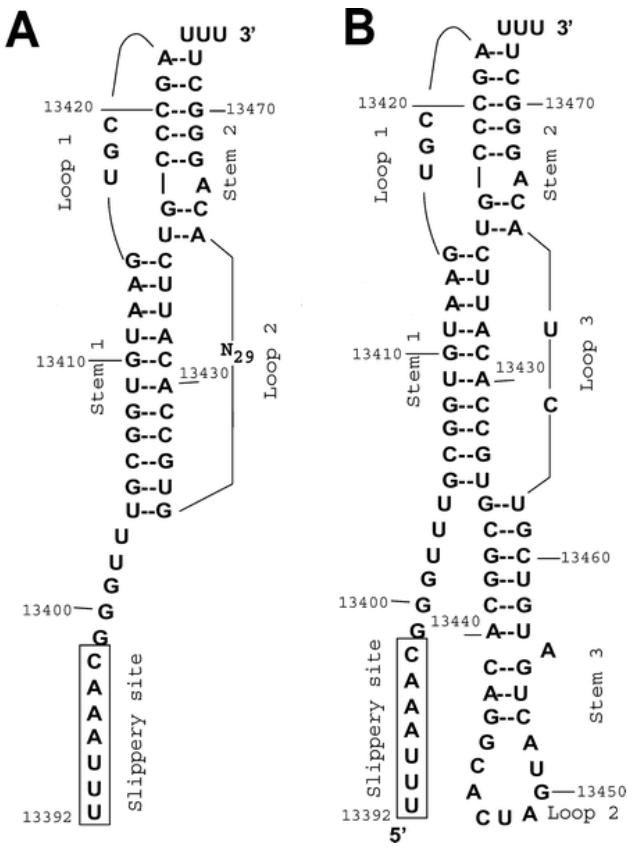

Figure 9. *Structure of SARS-CoV pseudoknot.* On the left is the original proposed structure of the SARS-CoV pseudoknot, while on the right is the accepted structure (Thiel et al, 2003; Plant *et al*, 2005). Take note of the stem and loop labels for future reference.

Chapter 3: Results

Part 1: SARS-CoV Frameshifting

To further glean information and insight into SARS-CoV frameshifting, a series of mutants were made in the frameshift signal. The first set of mutants examined the gross structure of the SARS-CoV pseudoknot, looking at each structural unit's contribution to frameshifting. Previous studies have already shown that changes to the slippery site change the frameshifting efficiency, as do changes to the distance between the slippery site and the pseudoknot (Baranov et al, 2005; Su *et al*, 2005).

Other structural studies have already pointed out some of the key structural elements of the pseudoknot. Total disruption of either stem 1 or stem 2 causes a ten to twenty- fold decrease in frameshifting (Baranov et al, 2005; Plant *et al*, 2005). Disruption of stem 3 seems to have a variable effect. Furthermore, there are two bulged As in the pseudoknot that seem to be important for frameshifting.

The first set of mutants examined stem 2, stem 3, loop 2, and the stem 2 bulged A, as seen in Figure 10. When the base pairing of stem 3 was disrupted, frameshifting was severely decreased. Then the structure of stem 3 was maintained, but certain base pairs were switched out. Frameshifting still decreased from 15.4% to 5.5%, suggesting that the sequence of stem 3 might be important and not just the structure. When loop 2 was mutated to an asymmetric loop, frameshifting decreased by approximately 30%. Furthermore, the unpaired adenosine in stem 2 was mutated

to a cytosine. Frameshifting consequently decreased to about 1.5%. This corresponds to another mutant where that nucleotide was deleted, which resulted in almost no frameshifting (Plant *et al,* 2005). Finally, stem 2 base pairing was interrupted and abolished frameshifting. This is also in agreement with what was reported by Plant *et al* (2005).

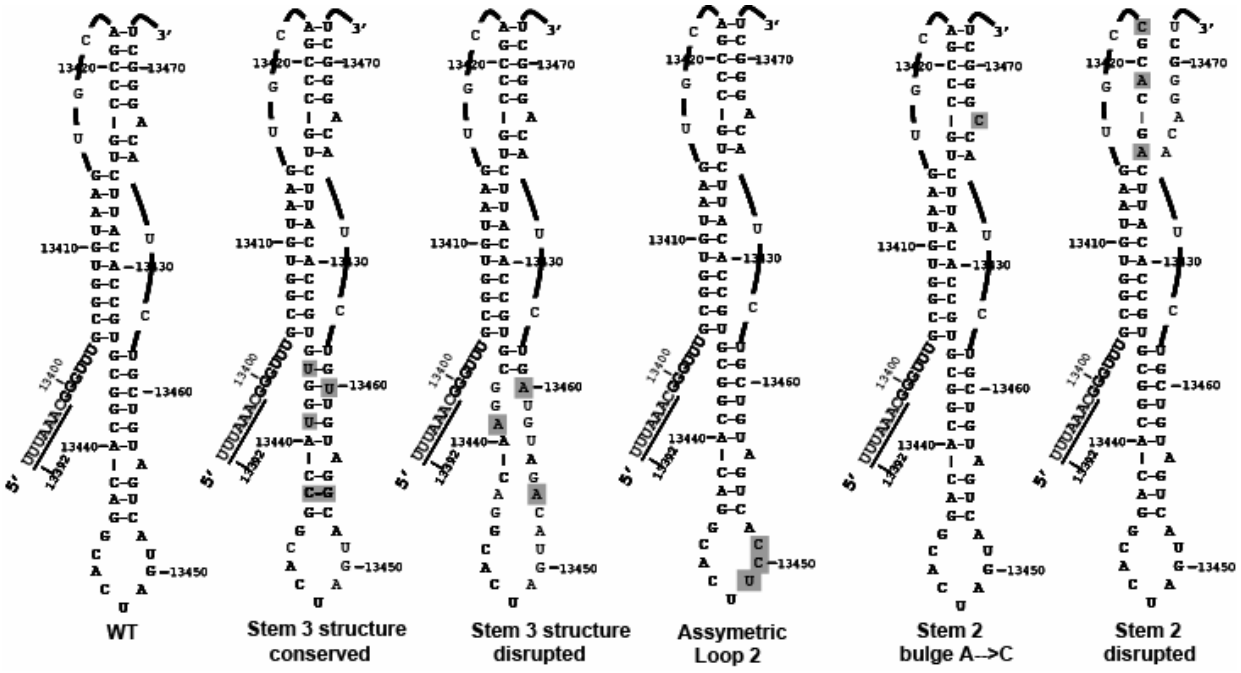

% PRF	15.4	5.50	2.78	4.66	1.43	0.38
St. Err.	0.455	0.1897	0.1003	0.1512	0.0663	0.0307

Figure 10. *Gross structural mutations in the SARS-CoV pseudoknot.* Mutations are highlighted by gray boxes. The frameshifting efficiency is denoted by %PRF and percent standard error is reported underneath the construct designation. Data was collected in two individual experiments until a normal distribution was established, allowing statistical analyses across and between experiments (Jacobs & Dinman, 2004).

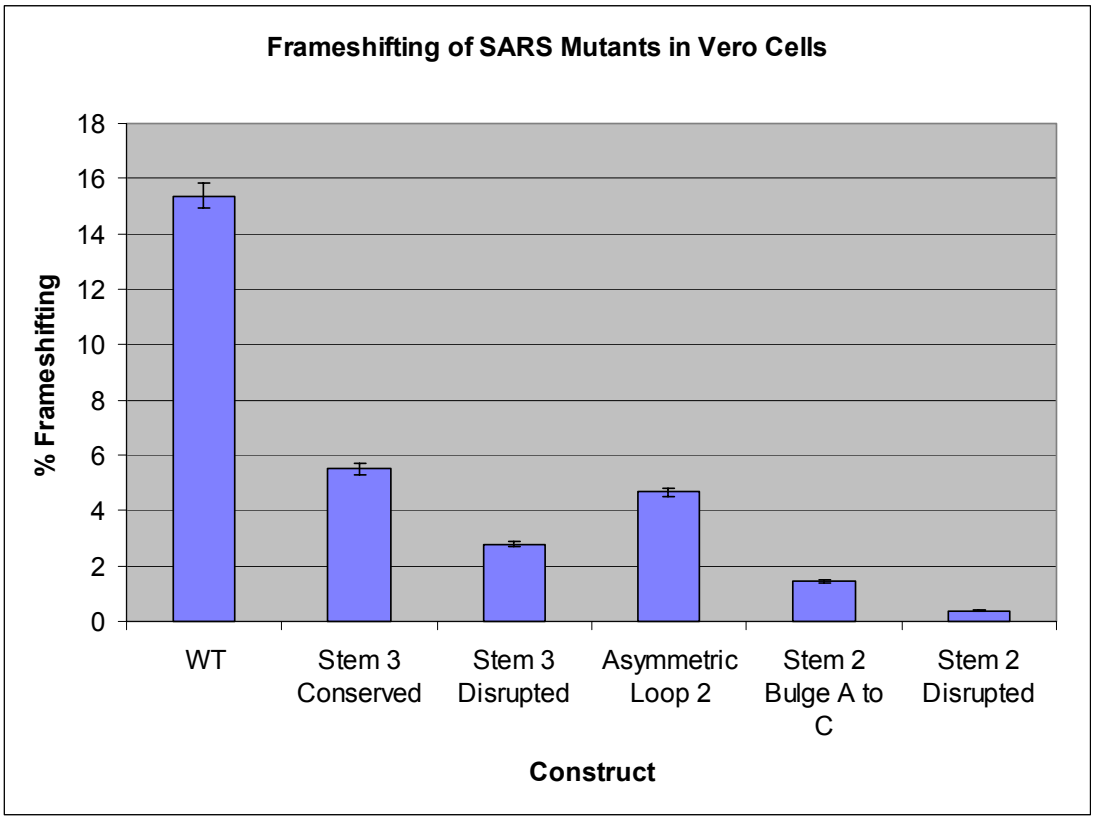

Figure 11. *Frameshifting of gross structural mutants in the SARS-CoV pseudoknot.* Absolute values of frameshifting efficiencies are graphed for comparison. Error bars denote percentage standard error.

The effect of loop 2 mutations and the change in frameshifting efficiency caused by the bulged A's required further investigation, as evidenced by Figure 10. It was noticed that the symmetric loop 2 allowed base pairing with another loop 2, as in a kissing loop interaction. This could be influential in frameshifting. Therefore, loop 2 was mutated to a tetraloop, which prevents the possible kissing loop interaction, as well as increases the stability of the pseudoknot. Increased stability would be

predicted to increase the amount of frameshifting due to further resistance to ribosome unwinding.

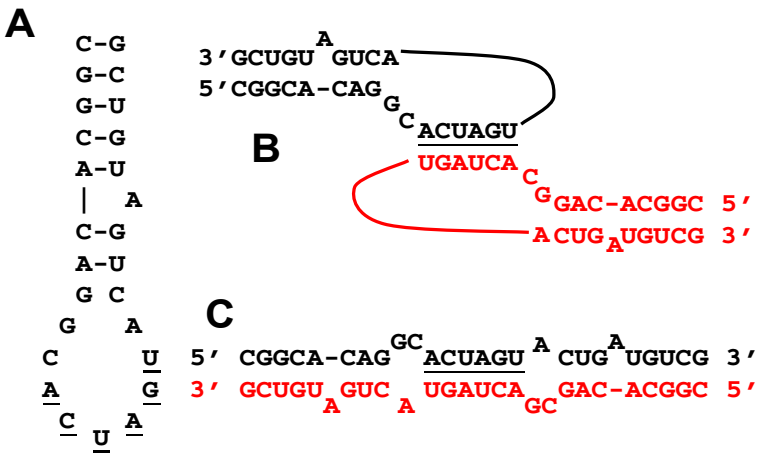

Figure 12. *Possible kissing loop interaction between two SARS-CoV pseudoknots.* Panel A shows the loop 2 of SARS-CoV pseudoknot. Panel B demonstrates the possible base pairing between two loop 2s, while Panel C shows extended base pairing between pseudoknots.

As previously mentioned, there are two bulged A's that seem to be important for frameshifting. When the stem 2 unpaired adenosine was either deleted or mutated to a C, frameshifting was negligible (Plant *et al*, 2005). More deletions were made of these unpaired bases, separately and in conjunction with each other. Depictions of these mutants can be seen in Figure 13. The loop 2 mutations were also generated with deletions of the bulged As. Another SARS-CoV mutant was made that investigated the importance of pseudoknot stability. Stem 3 was shortened to only two base pairs and loop 2 was replaced with a tetraloop. This should increase the overall stability of the pseudoknot, and would be predicted to increase frameshifting like the loop 2 mutant.

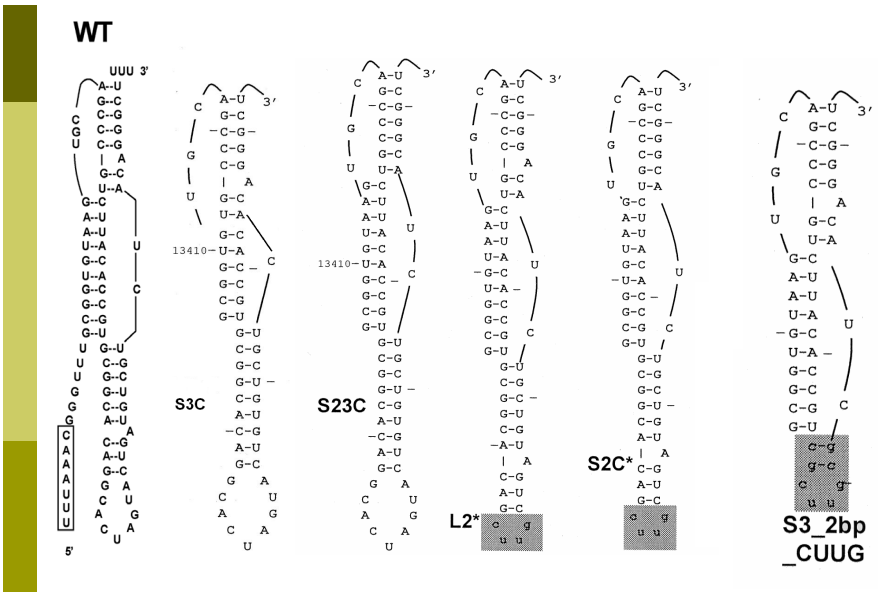

	WT	S3C	S23C	L2*	S2C*	S3_2bp _CUUG
% PRF	15.60	20.44	1.47	18.77	8.75	12.99
St. Err	0.10	0.671	0.077	0.170	0.437	0.545

Figure 13. *SARS-CoV pseudoknot mutants looking at deleted bulged adenosines or pseudoknot stability.* Mutated bases are highlighted by gray boxes, whereas deleted bulged As are not depicted. Frameshifting efficiency is denoted by % PRF and standard error is shown. Data was collected in four individual experiments until a normal distribution was established, allowing statistical analyses across and between experiments (Jacobs & Dinman, 2004).

These mutations had a broad range of effects on frameshifting. When the unpaired adenosine was deleted from S3C frameshifting increased by about 30%. However, when both unpaired adenosines were deleted, in the S23C mutant, frameshifting dropped to about 1.5%. This could mean that only the stem 2 bulged A is important, but further investigation is needed. The stable tetraloop that was made in loop 2 (L2*) showed increased frameshifting, which correlates to mRNA stability. Another mutant had the tetraloop and the stem 2 unpaired nucleotide deleted, S2C*, and frameshifting was about half of wildtype level. The shortened stem 3 with a

tetraloop, S3_2bp_CUUG, had a frameshifting efficiency of 13%, which was close to wildtype.

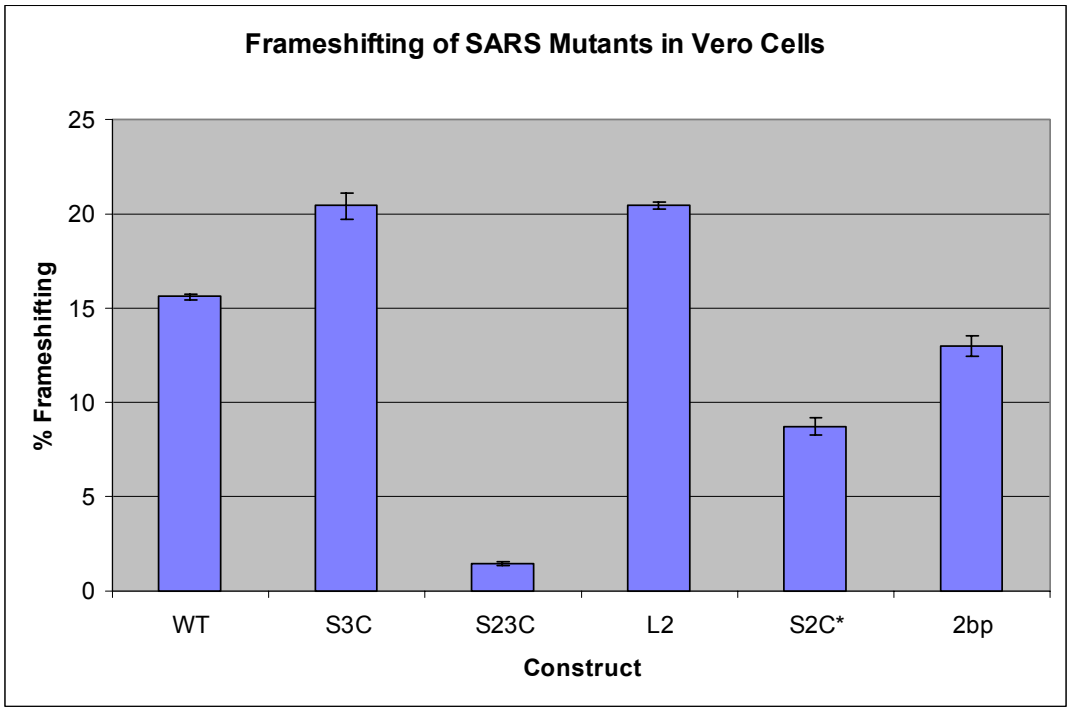

Figure 14. *Frameshifting effects of deleted unpaired adenosines and mRNA stability in the SARS-CoV pseudoknot.* Absolute values of frameshifting efficiencies are graphed for comparison. Error bars denote percentage standard error.

One group of investigators found that SARS-CoV has a so-called attenuator region upstream of the frameshift signal. It was discovered by including an additional 150 bases 5' of the pseudoknot into their dual luciferase construct. When they measured frameshifting, they found that frameshifting decreased by about 50% in comparison to the wildtype construct that contained just the frameshift signal (Su *et al*, 2005). It was then proposed that this highly structured region might somehow interact with the ribosome or downstream sequence to attenuate frameshifting efficiency.

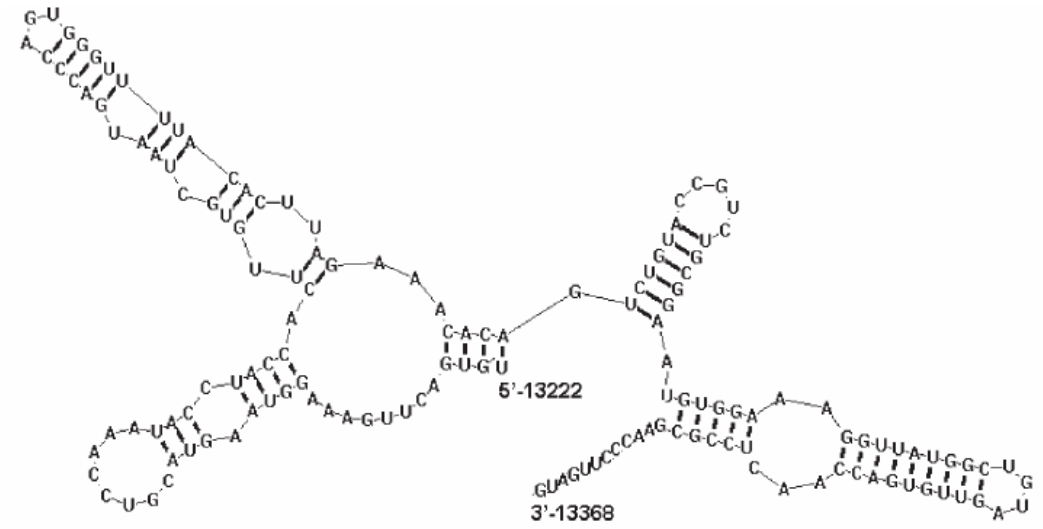

B

```
   C   D   L   K   G   K   Y   V   Q   I   P   T   T   C   A   N   D   P
5'TGT GAC TTG AAA GGT AAG TAC GTC CAA ATA CCT ACC ACT TGT GCT AAT GAC CCA
  C                   A               C       A   C       A       T

  V   C   F   T   L   R   N   T   V   C   T   V   C   G   M   W   K   G
 GTG GGT TTT ACA CTT AGA AAC ACA GTC TGT ACC GTC TGC GGA ATG TGG AAA GGT
  C   C       C           T       G               T   C       T       C

  Y   G   C   S   C   D   Q   L   R   E   P   L   M
 TAT GGC TGT AGT TGT GAC CAA CTC CGC GAA CCC TTG ATG 3'
      A           C   T           A
```

Figure 15. *SARS-CoV attenuator region and sequence.* The top panel shows the predicted structure of the attenuator region, located 150 bases 5' of the frameshift signal. Panel B displays the nucleotide sequence of the attenuator, with the amino acid sequence designated above with single letter abbreviations. Underneath the sequence, nucleotide substitutions are written that would affect base pairing in the attenuator, but preserve the amino acid sequence.

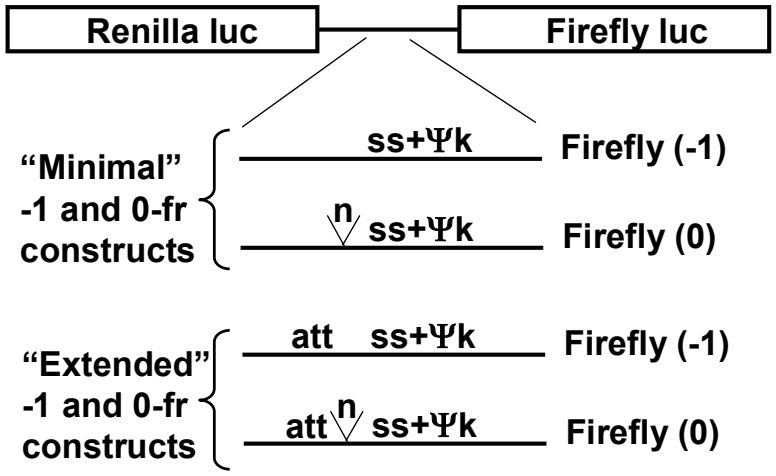

Figure 16. *SARS-CoV pseudoknot and attenuator constructs*. The minimal constructs contained just the SARS-CoV frameshift signal in the dual luciferase vector. The extended construct contains the frameshift signal and the upstream attenuator region as described by Su *et al* (2005). An extra base was added to 0 frame constructs so that the firefly luciferase gene is in the same reading frame as the renilla luciferase gene.

Test (-1 frame) renilla/ firefly ratio	Control (0 frame) renilla/ firefly ratio	Percent Frameshifting
Minimal -1 frame	Minimal 0 frame	15.2%
Extended -1 frame	Extended -1 frame	9.68%
Extended -1 frame	Minimal 0 frame	6.57%

Table 1. *SARS-CoV attenuator frameshifting*. The previous attenuator studies by Su *et al* (2005) calculated frameshifting efficiency by dividing the extended -1 frame by the minimal 0 frame. This is an inappropriate control and thus lowers the measured frameshifting efficiency.

When the extended construct of both the attenuator and SARS-CoV frameshift signal was tested, frameshifting was measured at 9.68%. This was approximately 60% of wildtype without the attenuator. Therefore, there was a difference observed, but not as much as previously reported.

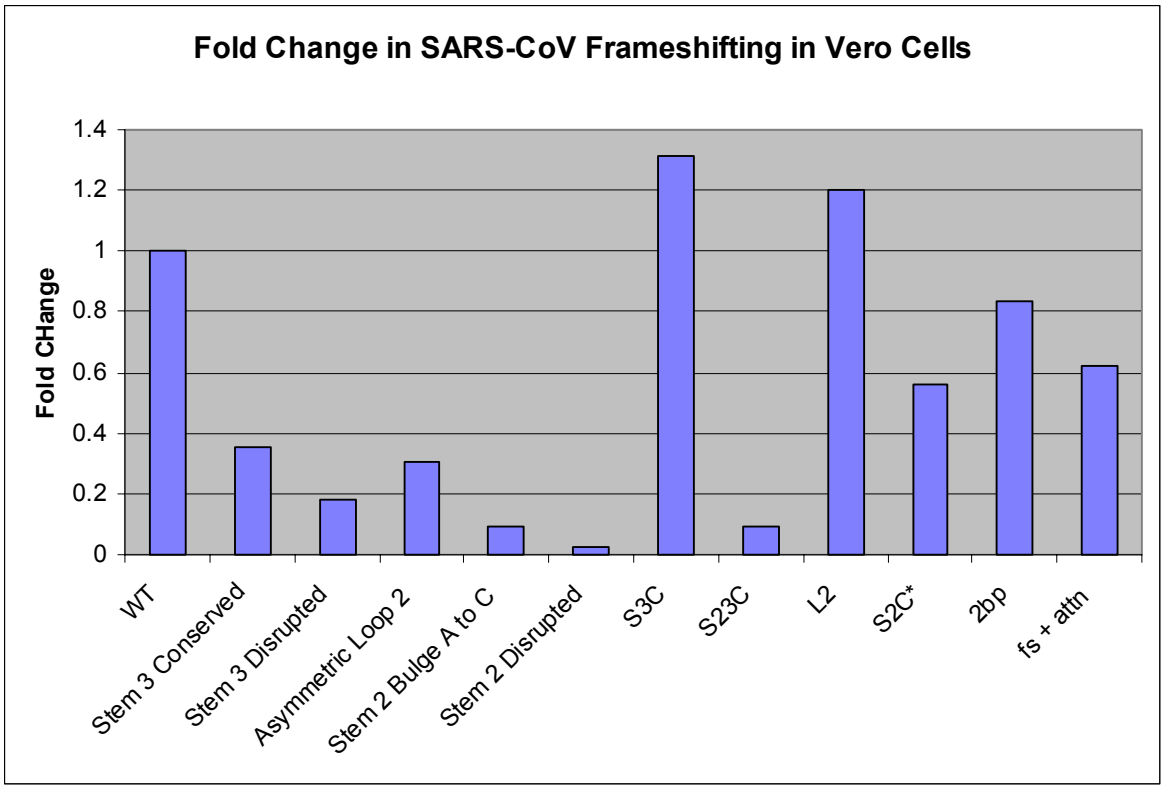

Figure 17. *Summary of SARS-CoV mutants and constructs*. The fold change of all the pseudoknot mutants and constructs are reported as normalized to the wildtype SARS-CoV frameshifting efficiency. The extended construct with the attenuator region is labeled as "fs + attn".

Part 2: Gentamicin's Influence on Frameshifting

Gentamicin is an aminoglycoside antibiotic that binds to the A site of the small subunit. Aminoglycosides increase misreading and prevent translocation from occurring (Davies & Davis, 1968). Gentamicin and other aminoglycosides stabilize the tRNA and mRNA interaction by flipping out the bases A1492 and A1493, which mimics cognate tRNA binding (Karimi and Ehrenberg, 1994; Yoshizawa *et al*, 1998). This prohibits proofreading of near-cognate aa-tRNAs.

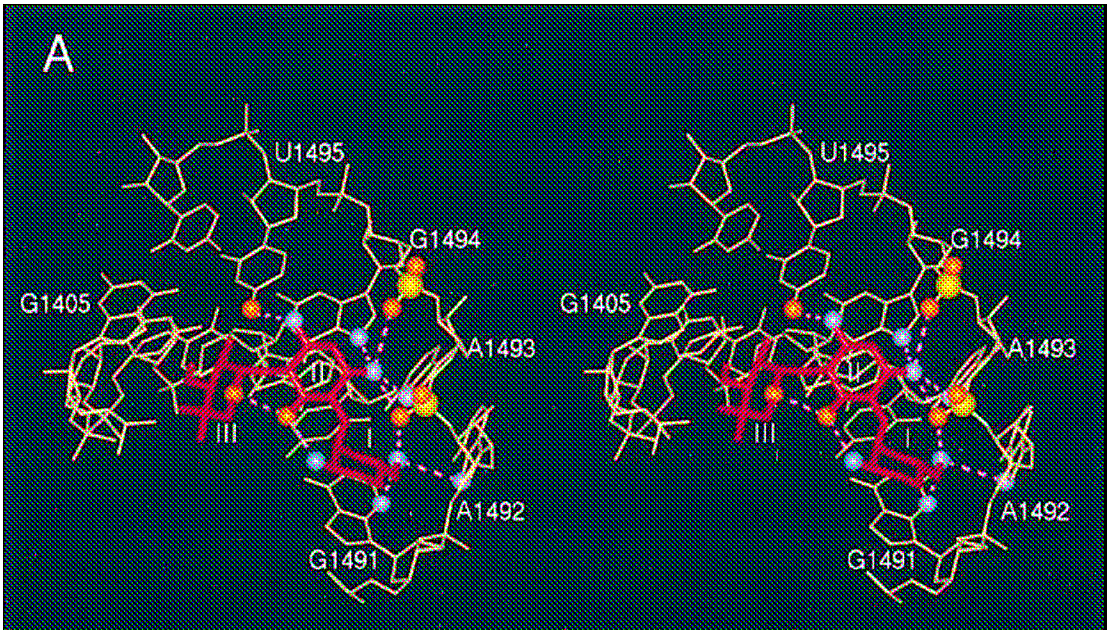

Figure 18. *Binding of gentamicin to the A site of the ribosome*. The antibiotic gentamicin is shown in red with the rRNA in beige. Interactions between the rRNA and gentamicin are highlighted (Yoshizawa *et al*, 1998).

Gentamicin has been approved for clinical use by the FDA to treat bacterial infections. It is also used to prevent microbial contamination in cell culture.

Here various amounts of gentamicin were used to culture HeLa CD4+ and Jurkat cells. The recommended concentration of gentamicin for use in cell culture is 50 mg/L (Sigma Aldrich). This was denoted a "1x" concentration, which was tested in conjunction with no gentamicin, 0.1x, 0.5x, 5x, and 10x concentrations. The actual amounts of gentamicin are reported in the following figures. Furthermore, the read-through control was also measured at each gentamicin concentration in each cell line, and used to calculate the percent frameshifting for individual values.

The frameshifting efficiencies of both HIV and SARS-CoV were measured by dual luciferase assays. There was a general trend of increased frameshifting with increasing amounts of gentamicin. Overall, HIV frameshifting increased from about 2.4% without gentamicin to 4% with 500 mg/L of gentamicin in HeLa CD4+ cells. SARS-CoV frameshifting increased from 12.8% to 17.2% overall, a total of 4.5% in the same cell line.

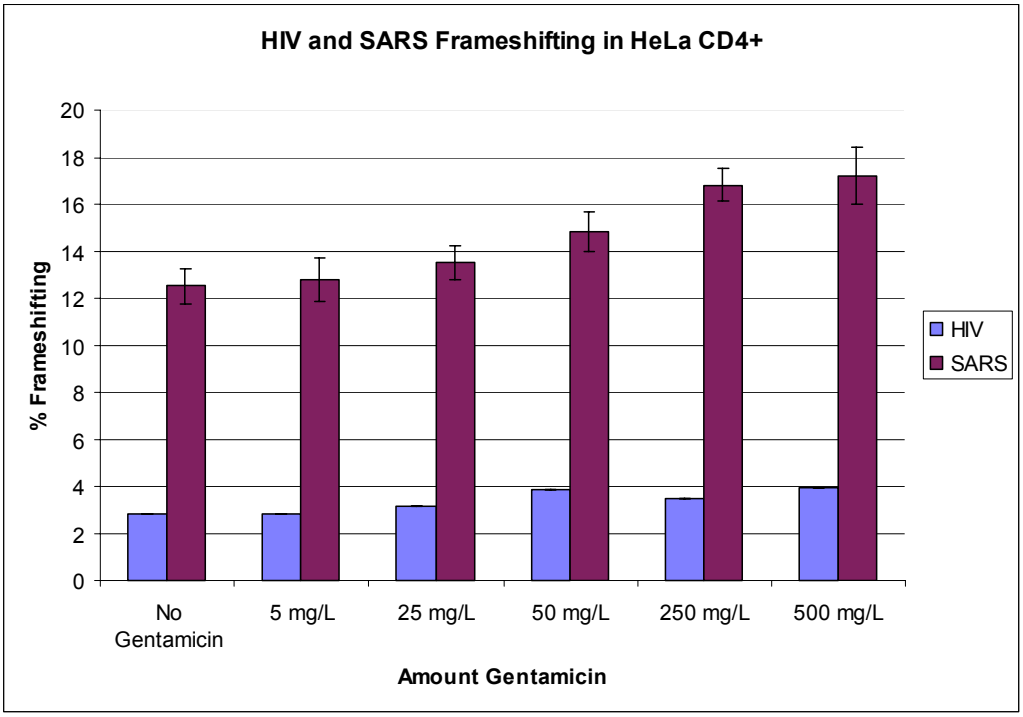

Figure 19. *Gentamicin affects on frameshifting of HIV and SARS-CoV in HeLa CD4+ cells.* Error bars denote percent ratiometric standard error. Data was collected in four individual experiments until a normal distribution was established, allowing statistical analyses across and between experiments (Jacobs & Dinman, 2004).

The same trend was seen in Jurkat cells. HIV and SARS-CoV frameshifting increased by approximately 20% with 500 mg/L gentamicin in comparison to a no gentamicin control. There is the pattern that frameshifting efficiency increases with

increasing amounts of gentamicin. Overall, in both cell lines, there is a total of up to 1.4-fold increase at the maximum concentration, i.e. an up to 40% increase in frameshifting compared to no drug controls.

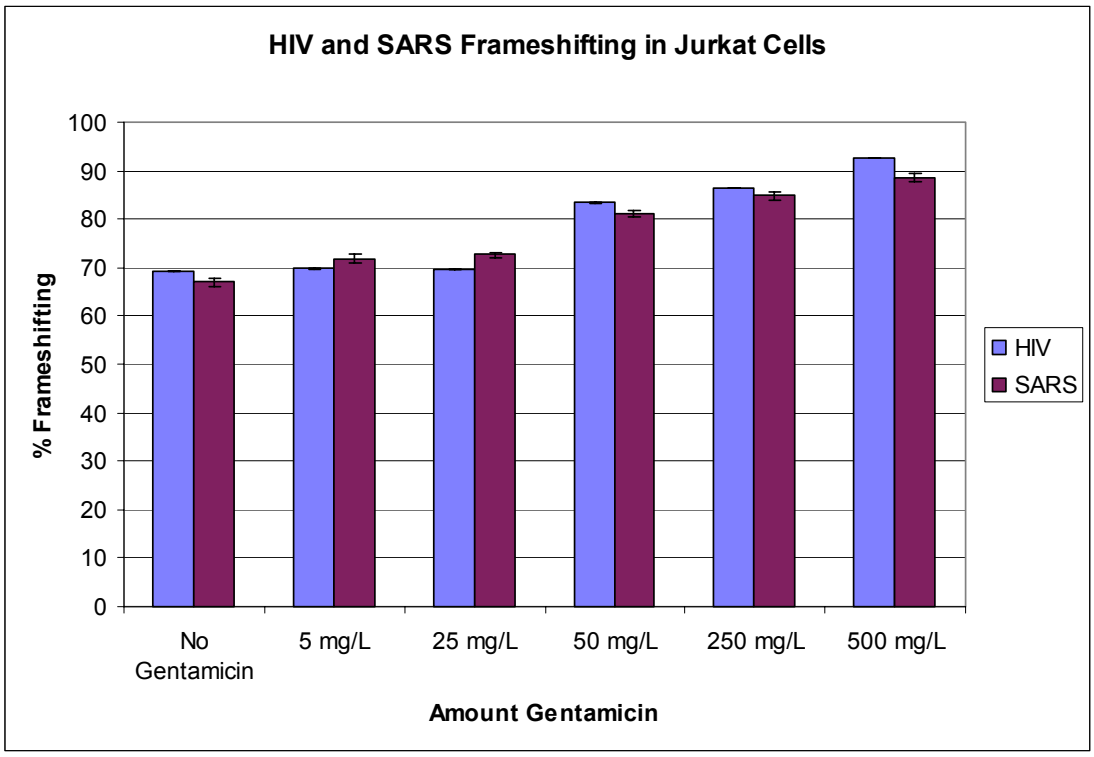

Figure 20. *Gentamicin affects on frameshifting of HIV and SARS-CoV in Jurkat cells.* Error bars denote ratiometric standard error. Data was collected in five individual experiments until a normal distribution was established, allowing statistical analyses across and between experiments (Jacobs & Dinman, 2004).

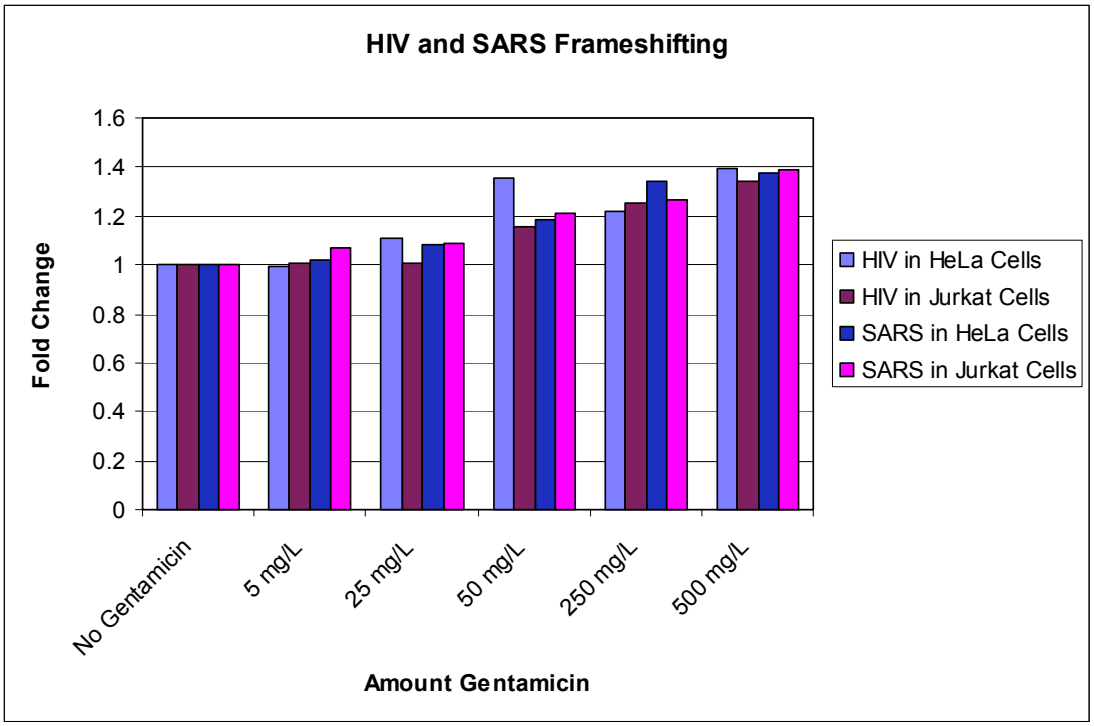

Figure 21. *Summary of gentamicin's effect on frameshifting.* Each frameshifting value was normalized to the wildtype frameshifting efficiency with no gentamicin in a particular cell type.

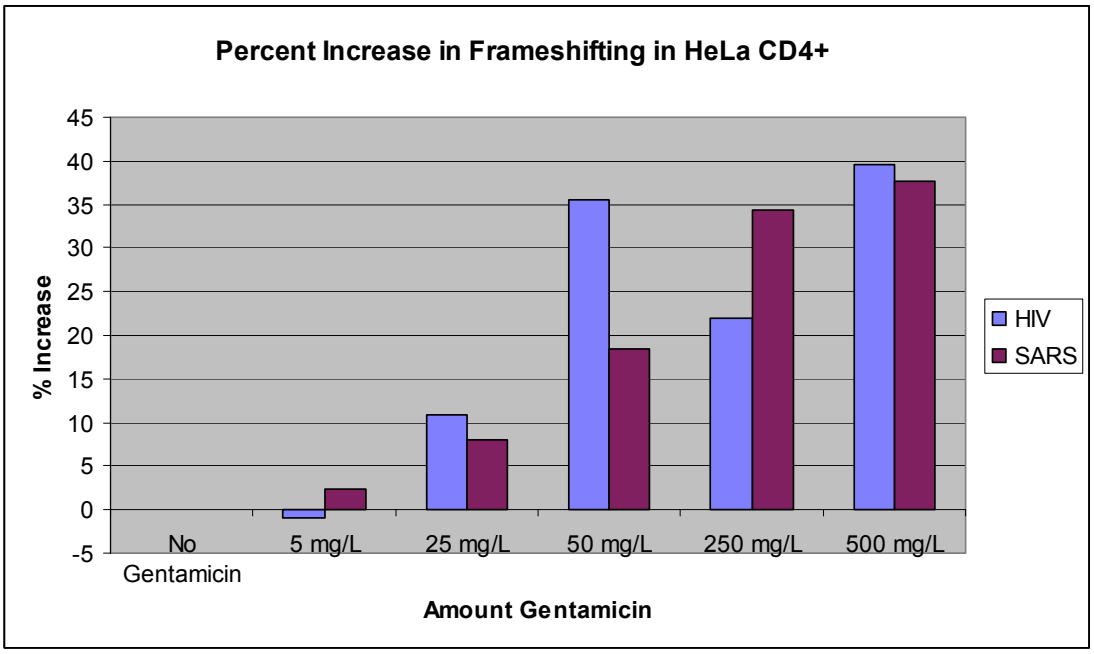

Figure 22. Percent increase in frameshifting in HeLa CD4+ cells.

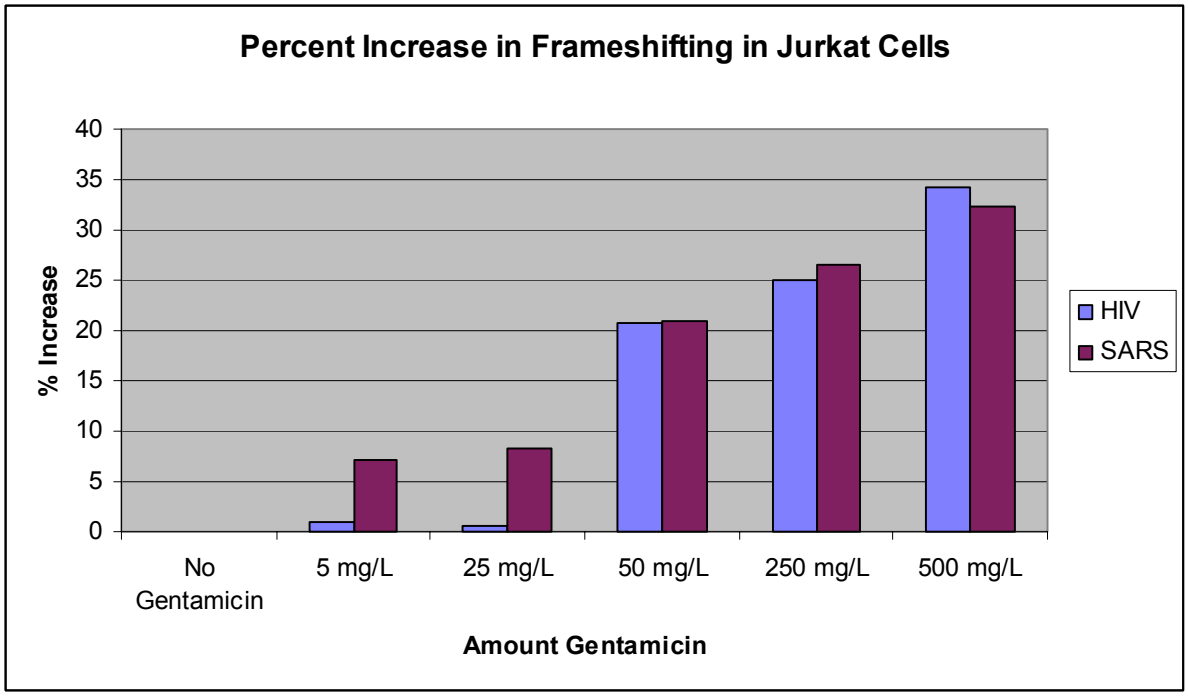

Figure 23. Percent increase in frameshifting in Jurkat cells.

Part 3: Frameshifting in CCR5

The human CCR5 gene is expressed in activated CD4+ T cells. The protein product is displayed on the surface of the cell and acts as a receptor for various chemokines. It is also the co-receptor for HIV, and required for infection. A potential frameshift signal was discovered in CCR5 by a computational program that examines sequences for potential frameshift signals.

The slippery site for CCR5 consists of U UUA AAA, and there is a strong downstream pseudoknot. Frameshifting would produce a truncated protein product because there is a stop codon in the -1 frame after the frameshift signal. The full length CCR5 protein has 352 amino acids, where the frameshift product is predicted

to be 226 amino acids. It is not known whether there are separate functions for the full length and truncated protein products.

The predicted -1 PRF CCR5 signal was cloned into a mammalian dual luciferase vector and frameshifting measured in Vero cells. It was found that this promoted frameshifting approximately 8.0% of the time. To further validate and analyze the frameshift signal, mutants were made that either disrupted the slippery site so frameshifting could not occur or disrupted base pairing in stem 2 of the pseudoknot. The slippery site was changed from U UUA AAA to C UUG AAG. In order to disrupt stem 2, the 5' side of the stem was mutated to the 3' side, and vice versa. This means the same sequence was on either side of the stem, preventing base pairing, as seen in Figures 25 and 26.

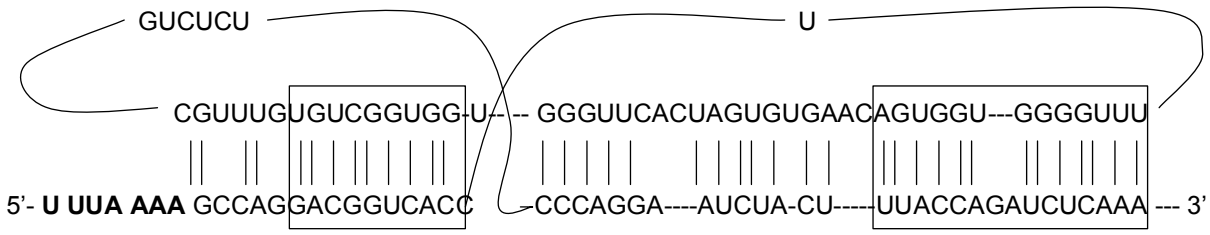

Figure 24. *Structure of the CCR5 frameshift signal.* The slippery site is highlighted in bold with spacing indicating the incoming reading frame. Stems 1 and 2 are boxed, with stem 1 being 5' in the pseudoknot and stem 2 being 3', respectively.

Changing the slippery site caused a decrease in frameshifting, as well as disrupting stem 2. The slippery site mutant frameshifted 1.3% of the time, which was a decrease of 83% over wildtype. The stem 2 5' mutant had a frameshifting efficiency of 1.9%, while the stem 2 3' was measured at 2.8%.

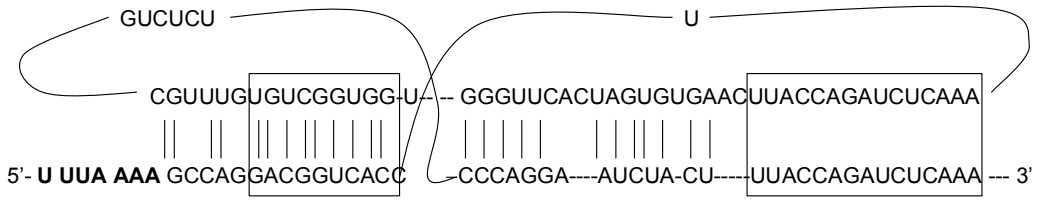

Figure 25. CCR5 mutant stem 2 5' complement.

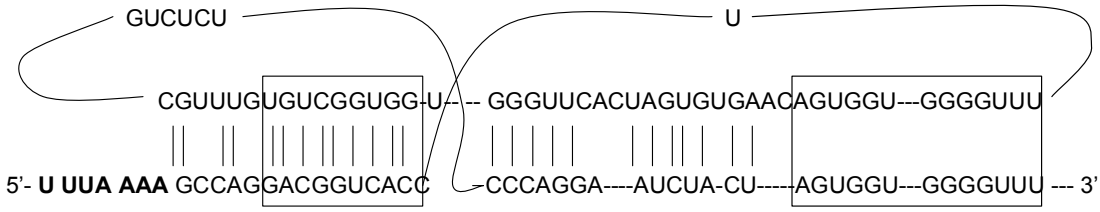

Figure 26. CCR5 mutant stem 2 3' complement.

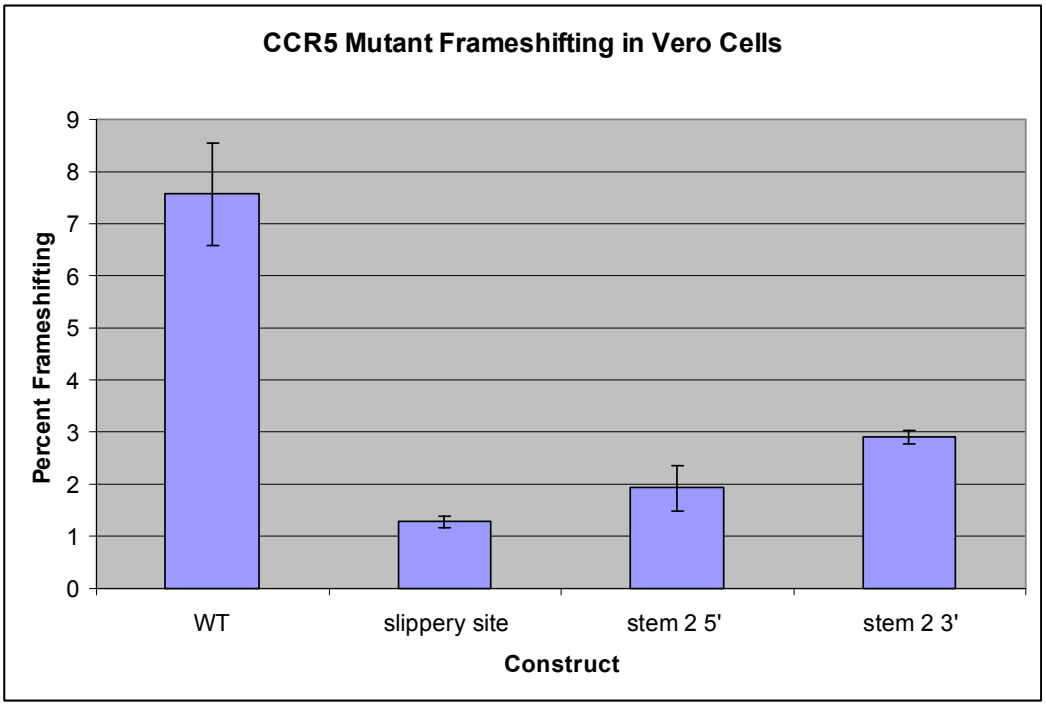

Figure 27. *Frameshifting efficiency in CCR5 constructs*. Error bars denote percent ratiometric standard error. Data was collected in two individual experiments until a

normal distribution was established, allowing statistical analyses across and between experiments (Jacobs & Dinman, 2004).

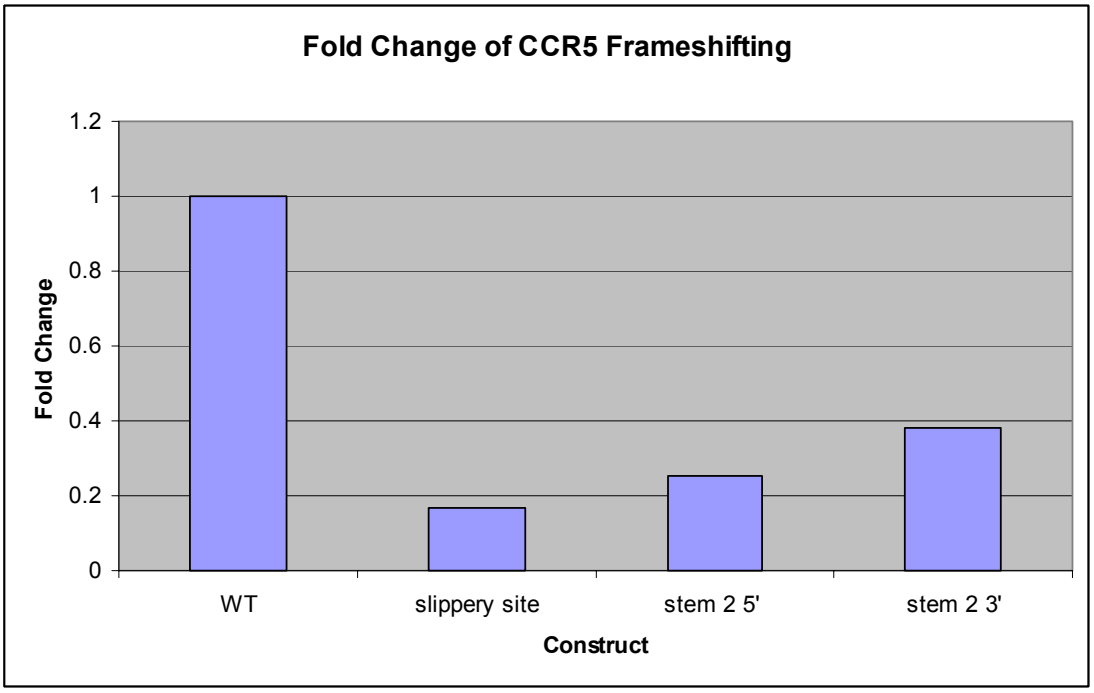

Figure 28. Fold change of CCR5 frameshifting values.

Chapter 4: Materials and Methods

HIV and SARS-CoV Wildtype Plasmids.

The SARS-CoV frameshift signal has been cloned into dual luciferase vectors as previously described in Plant et al (2005) as both a 0-frame control (pJD464) and a -1 test construct (pJD502). The HIV -1 PRF signal (pJD175c) and 0-frame control (pJD175d) used for dual luciferase assays in mammalian cells were previously reported by Grentzmann et al (1998).

Oligonucleotides, Plasmid Construction and Mutagenesis.

The first set of SARS-CoV mutants that included Stem 3 disrupted, Stem 3 conserved, Assymetric loop 2, Stem 2 Bulge A to C, and Stem 2 disrupted were all made previously by Dr. Ewan Plant (Dept. Cell Biology & Molecular Genetics, University of Maryland).

To generate the other SARS-CoV mutants, oligonucleotide site directed-mutagenesis was performed. Oligonucleotides were synthesized and purified from IDT (Coralville, Iowa). They are listed in Table 1.

The mutants L2, S3C, and 2 bp were generated by annealing oligonucleotides to the wildtype dual luciferase plasmid, pJD502, and amplified by PCR using the Stratagene QuikChange XL10 kit (La Jolla, California). The mutant plasmid, L2, was also used as template for generating the S2C* mutant. The mutant S23C used the template S2C (pJD473), which was generated previously as described (Plant *et al*, 2005).

After the initial changes were made in the SARS-CoV pseudoknot, some mutants required the insertion of additional bases to maintain the firefly luciferase gene in the -1 frame. This was done through oligonucleotide site-directed mutagenesis. S3C had one adenosine inserted immediately 3' of the pseudoknot by use of the "1 base frame" oligonucleotides, as did S23C using the "1 base frame with S2C" oligonucleotides. Another construct, 2 bp, needed two adenosines inserted downstream of the pseudoknot to maintain the -1 frame, which were inserted using the "2 base frame" oligonucleotides. The mutagenesis was performed using the Stratagene QuikChange XL10 kit (La Jolla, California) and amplified by PCR.

To make the extended constructs of the SARS-CoV attenuator and frameshift signal, the attenuator and frameshift region (13222-13520) was amplified by PCR out of pJD507 using DNA primers that contained SalI and SacI restriction sites. The resulting DNA fragment was digested with restriction enzymes SalI and SacI, as well as the mammalian dual luciferase vector pJD175f. These were ligated together and transformed into DH5α cells for maintenance and selection by carbenicillin. The resulting plasmid contained the attenuator and frameshift region with firefly in the 0 frame. The test construct with firefly in the -1 frame was produced by inserting an adenosine between the attenuator and frameshift signal using the "fs + attn -1" oligonucleotides and the Stratagene QuikChange XL10 kit.

The CCR5 wildtype construct was generated previously by Trey Belew (Dept. Cell Biology & Molecular Genetics, University of Maryland). The subsequent plasmid, pJD827, was used as template to make the slippery site, stem 2 5' complement, and stem 2 3' complement mutants. This was done by oligonucleotide

site-directed mutatgenesis using the Stratagene QuikChange XL10 kit and amplification by PCR. The slippery site mutant used the "CCR5 slip site" oligonucleotides, while the stem 2 5' and stem 2 3' used their respective oligonucleotides.

Table 2. Oligonucleotides Used in This Study

Name	**Sequence**
L2	5' ccgtcttacaccgtgcggcacaggCTTGcctgatgtcgtctac 3'
S3C	5' gcggcacaggcactagtacTGTgtcgtctacagggcttttgagc 3'
S23C	5' gcggcacaggcactagtacTGTgtcgtctACGggctatttgagc 3'
2 bp	5' gcagcccgtcttacaccgtCGCTTGCGctacagggcttttgagc 3'
S2C*	5' ggCTTGcctgatgtcgtctaCGggctAtttgagctcatggaagacgcc 3"
1 base frame	5' cctgtgtcgtctacagggctatttgagctcatggaagacgcc 3'
2 base frame	5' cgtCGCTTGCGctacagggctactttgagctcatggaagacgc 3'
1 base frame with S2C	5' gtacTGTgtcgtctACGggctactttgagctcatggaagacgcc 3'
Fs + attn -1	5' cgtctacagggcttttagagctcgaagacgccagaaaggc 3'
CCR5 slip site	5' cgactgtcgtccatgctgtgtttcggttgaaggccaggacggtcacctttgg 3'
CCR5 stem 2 5'	5' ccaggacggtcaccaaactctaccattcaagtgtgatcacttgggtggtggc 3'
CCR5 stem 2 3'	5' gcgtctgtcccaggaatcatcttagtggtgaggggtttaagaaggtcttcattacacc 3'

SARS-CoV and CCR5 Mutant Frameshifting Assays.

African green monkey Vero cells were plated at a concentration of 3.0 x 10^5 cells/mL in a 24-well plate. The cells were cultured in DMEM supplemented with 10% FBS and without antibiotics at 37ºC with 5% CO_2. The following day the cells were transiently transfected with 1 µg of plasmid DNA using 2 µl ExpressFect (Denville Scientific) per well following manufacturer's directions.

After 24 hours, Vero cells were washed with PBS and lysed with 1x Passive Lysis Buffer (Dual-Luciferase Reporter System, Promega) with gentle rocking for fifteen minutes. A Turner 20/20 luminometer was used to measure renilla and firefly luciferase activity (Dual-Luciferase Reporter System, Promega, Fitchburg, Wisconsin, United States). Transfections were performed in triplicates with at least three luciferase readings from each transfection. Data was collected until a normal distribution was established, allowing statistical analyses across and between experiments (Jacobs & Dinman, 2004).

Frameshifting percentage was calculated by dividing the test construct renilla to firefly ratio by the control renilla to firefly ratio, and then multiplying by one hundred.

Gentamicin Frameshifting Assays.

HeLa CD4+ cells were plated at a concentration of 3.0 x 10^5 cells/mL and Jurkats at a concentration of 4.0 x 10^5 cells/mL in a 24-well plate. The cells were cultured in DMEM supplemented with 10% FBS and increasing amounts of gentamicin sulfate (Sigma Aldrich) at 37ºC with 5% CO_2. The following day the cells

were transiently transfected with 1 µg of plasmid DNA using 2 µl ExpressFect (Denville Scientific) per well following manufacturer's directions.

After 24 hours, HeLa CD4+ cells were washed with PBS and lysed with 1x Passive Lysis Buffer (Dual-Luciferase Reporter System, Promega) with gentle rocking for fifteen minutes. Jurkat cells were harvested by centrifugation at 1000x g for five minutes. The pellet was washed with PBS, and then cells were lysed by resuspension in 1x Passive Lysis Buffer. A Turner 20/20 luminometer was used to measure renilla and firefly luciferase activity (Dual-Luciferase Reporter System, Promega, Fitchburg, Wisconsin, United States). The read-through control and the test construct were measured at each of the gentamicin concentrations. Transfections were performed in triplicates per amount of gentamicin used with at least three luciferase readings from each transfection. Data was collected until a normal distribution was established, allowing comparison across and between experiments.

Frameshifting percentage was calculated by dividing the test construct renilla to firefly ratio at a specific gentamicin concentration by the control renilla to firefly ratio at the same gentamicin concentration, and then multiplying by one hundred.

Chapter 5: Discussion

Part 1: SARS-CoV Frameshifting

A series of mutants were made to investigate the important features of the SARS-CoV pseudoknot, as evidenced in Figure 10. Disruption of Stem 2 resulted in nearly abolished frameshifting. The base pairing of stem 3 was disrupted and then re-established with different base pairs. When there was no base pairing in stem 3, frameshifting was significantly decreased. However, after reforming the stem with a new sequence, frameshifting was only a third of wildtype. This suggests that the sequence of stem 3 is important for frameshifting efficiency, and not just the structure of stem 3 itself. Moreover, when stem 3 was shortened from nine base pairs to only two base pairs and loop 2 was mutated to a tetraloop, as in the 2 bp mutant, frameshifting was measured at 13%. This is about 80% of wildtype. In this construct, the importance of the stem 3 sequence for frameshifting could be off set by the increased stability of the shortened stem with a tetraloop, as it has previously been known that increased mRNA stability leads to increased frameshifting (Namy *et al*, 2006).

Loop 2 was mutated to an asymmetric loop. Frameshifting decreased to 30% of wildtype. Also, loop 2 was mutated to a tetraloop that would increase the stability and frameshifting also increased by 2% as a result (Figure 13). It is interesting to note that there is the possibility of loop 2 to form a kissing loop interaction with another loop 2, as referenced in Figure 12. Both the asymmetric loop and the L2* construct

would prevent this possible interaction. In the case of L2*, the increased stability of the tetraloop could balance out the detrimental effects of preventing the kissing loop interaction. However, it is also possible that the bases mutated to form the asymmetric loop were themselves important for frameshifting. It has not yet been shown whether this kissing loop interaction actually takes place *in vivo* or whether it is truly important for frameshifting. Further experiments need to be done to determine this.

Another interesting feature of the SARS-CoV pseudoknot is the two unpaired adenosines in stem 2 and stem 3. These have been hypothesized to be important for frameshifting efficiency. When the stem 2 bulged A was mutated to a C or deleted, frameshifting dropped to between one and two percent (Plant *et al*, 2005). When both bulged As were deleted, frameshifting decreased to a similar level. On the other hand, when the stem 3 unpaired adenosine was singularly deleted, frameshifting actually increased. This can be seen in Figure 13. Overall, it seems that the stem 2 bulged A is important for frameshifting efficiency and certainly more important than the stem 3 bulged A.

This is further validated by the construct S2C*, in which loop 2 is mutated to a stable tetraloop and the stem 2 unpaired adenosine is deleted. The frameshifting efficiency was measured at 13%, similar to wildtype. The increased stability of the mRNA from the tetraloop could off set the decrease in frameshifting caused by the deleted bulge A.

Further mutational analyses should be done to validate these findings. Suggested constructs are drawn below in Figure 29. S3C* would look at the stem 3

unpaired adenosine and mRNA stability with the tetraloop. S23C* would have both unpaired adenosines deleted and have loop 2 mutated to a tetraloop. Finally, S3_4bp_UUCG would have a shortened stem 3 with only four base pairs compared to the wildtype stem 3 with 9 base pairs, and have a tetraloop. This would increase the mRNA stability of the pseudoknot. Also, part of the sequence of stem 3 would be conserved in S3_4bp_UUCG, looking at what bases are important for frameshifting efficiency.

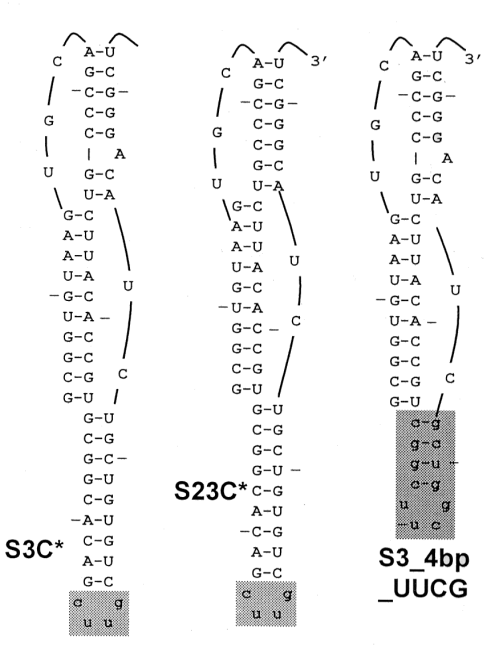

Figure 29. *Suggested additional mutants of the SARS-CoV pseudoknot*. These constructs further investigate the importance of the unpaired adenosines, mRNA stability, the possible kissing loop interaction, and the sequence of stem 3.

One study had shown that there was a possible upstream attenuator region in the SARS-CoV genome. The attenuator is a highly structured region that is approximately 150 bases upstream from the frameshift signal. It was found that when this region is included in constructs looking at frameshifting efficiency, frameshifting

decreased by 50%. When this experiment was repeated, frameshifting was 60% of the wildtype level without the attenuator region.

How, and if, the attenuator actually impacts frameshifting remains to be investigated. It could be that the attenuator is interacting with the ribosome or pseudoknot directly, or a protein factor is binding and affecting frameshifting. However, it could be that the attenuator is acting as a "translational speed bump," where ribosomes are falling off when translating the mRNA due to the secondary structure. The upstream reporter would be consistently translated, but the downstream reporter would be translated less, which would look like a decrease in frameshifting efficiency. This could be examined by mutating the attenuator region by disrupting base pairing, shown in Figure30. Reducing the secondary structure could keep more ribosomes on, and also look at whether the structure or nucleotide sequence is important.

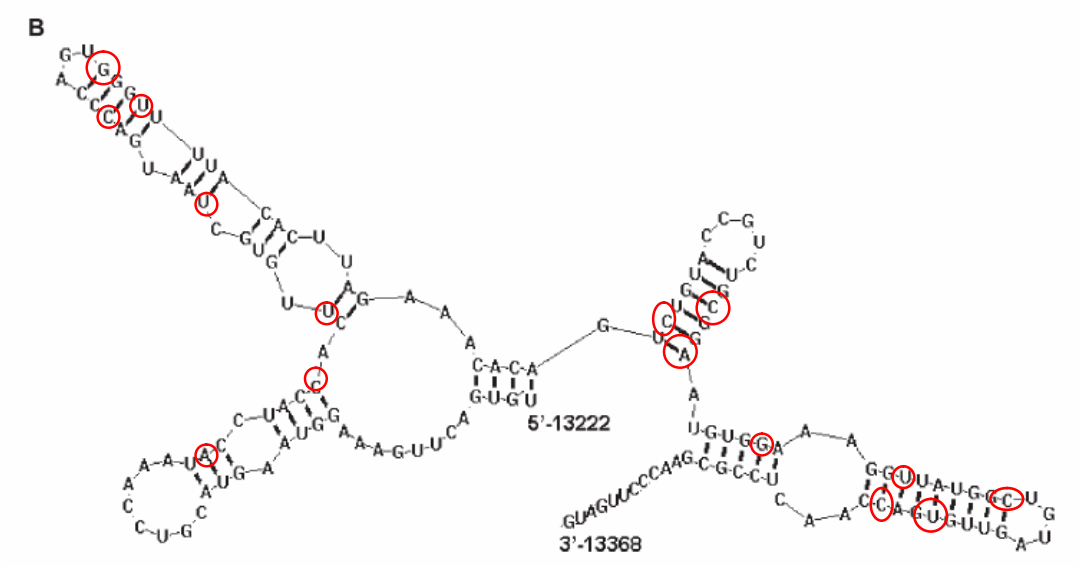

Figure 30. *Suggested mutations in the SARS-CoV attenuator region*. The bases that are circled in red are bases that can be mutated to disrupt base pairing while maintaining the same amino acid sequence.

From the mutants already made, it can be determined that the important features of the SARS-CoV pseudoknot include: the sequence of stem 3, loop 2, and the stem 2 bulged A. Future work should investigate the existence of the kissing loop interaction of loop 2 or base pairing between SARS-CoV pseudoknots should be investigated. It would also be informative to separate the disruption of the possible kissing loops with mRNA stability, and to study these individually.

Part 2: Gentamicin's Influence on Frameshifting

Aminoglycosides are antibiotics that bind to the A site of the ribosome. These can decrease translational fidelity by stabilizing near-cognate binding in the A site, and also increase programmed ribosomal frameshifting by stabilizing base pairing in the -1 frame. Moreover, disrupting frameshifting efficiency can have dramatic impacts on viral propagation (Dinman & Wickner, 1992; Léger *et al*, 2007).

When the aminoglycoside gentamicin was added to media in increasing concentrations, the frameshifting efficiency of both HIV-1 and SARS-CoV increased over a no gentamicin control. There was a 1.4-fold increase in HIV frameshifting in HeLa CD4+ cells with 500mg/L gentamicin, shown in Figure 19. SARS-CoV frameshifting increased from about 12.5% to 17.5%. In Jurkat cells, HIV frameshifting increased 34% and SARS-CoV increased by 32% compared to without gentamicin (Figure 20). Overall, with increasing gentamicin concentrations there is increasing ribosomal frameshifting.

This study is in collaboration with other laboratories who are investigating gentamicin's effect on viral propagation. HIV results correlated well with the

frameshifting assays. As the efficiency of frameshifting increased, infectivity decreased. This was measured by reverse transcriptase assays and viral titers.

Gentamicin is a drug approved by the FDA to treat bacterial infections. About ten percent of the population experience major side effects that include problems with kidneys and the inner ear. Physicians typically prescribe a dose of 5-7 mg/kg, which is about twice the maximum concentration of gentamicin used in the frameshifting and viral propagation studies.

Gentamicin, then, could theoretically be used as a new treatment for HIV. It is safe for most of the human population and decreases viral titer. Gentamicin decreases translational fidelity, and is supposed to be specific to bacterial ribosomes. However, this study saw an effect with eukaryotic ribosomes in cell culture.

Further investigation into using gentamicin clinically needs to be done. Other aminoglycosides should also be examined. This study has pointed out a specific binding site that could be used as an antiviral target.

Another facet of this study is the different mechanisms that frameshifting affects. In HIV, changing the frameshifting efficiency causes assembly defects, due to the different stoichiometry between gag, the structural protein, and pol, the enzymatic proteins. However, in SARS-CoV, the frameshift signal controls the ratio between different enzymatic proteins. It is not fully understood how changing the frameshifting efficiency effects viral propagation. This is something that needs to be studied, and could also lead to another antiviral therapy.

Part 3: Frameshifting in CCR5

CCR5 is a human chemokine receptor that is present on the surface of several types of immune cells. It is also the co-receptor of HIV, and required for entry of the virus into the cell. A frameshift signal was predicted to be located within the human gene of CCR5. When this was cloned into a dual luciferase reporter, it was found that the -1 PRF signal was functional.

Further mutational analysis was done to validate the frameshift signal. The slippery site was mutated from U UUU AAA to C UUG AAG. This prevents base pairing in the -1 frame so frameshifting cannot occur. Also, stem 2 was disrupted by mutating the 5' side of the stem to the 3' side (Figure 25). That means the same sequence was on each side of the stem, completely preventing base pairing. This was also done to the 3' side (Figure 26). By disrupting stem 2, the stability of the pseudoknot decreases and thus frameshifting decreases.

Future studies should include other mutants to examine the CCR5 frameshift signal. Stem 1 should be disrupted in the same way that stem 2 was, as shown in Figure 31. Also, compensatory mutations should be made that restore base pairing in the stem, but reverse the sequence. For example, the wildtype 5' sequence should be on the 3' side and the 3' sequence on the 5' side. This will determine if the structure itself or the sequence is important for frameshifting efficiency. This should be done for both stem 1 and stem 2.

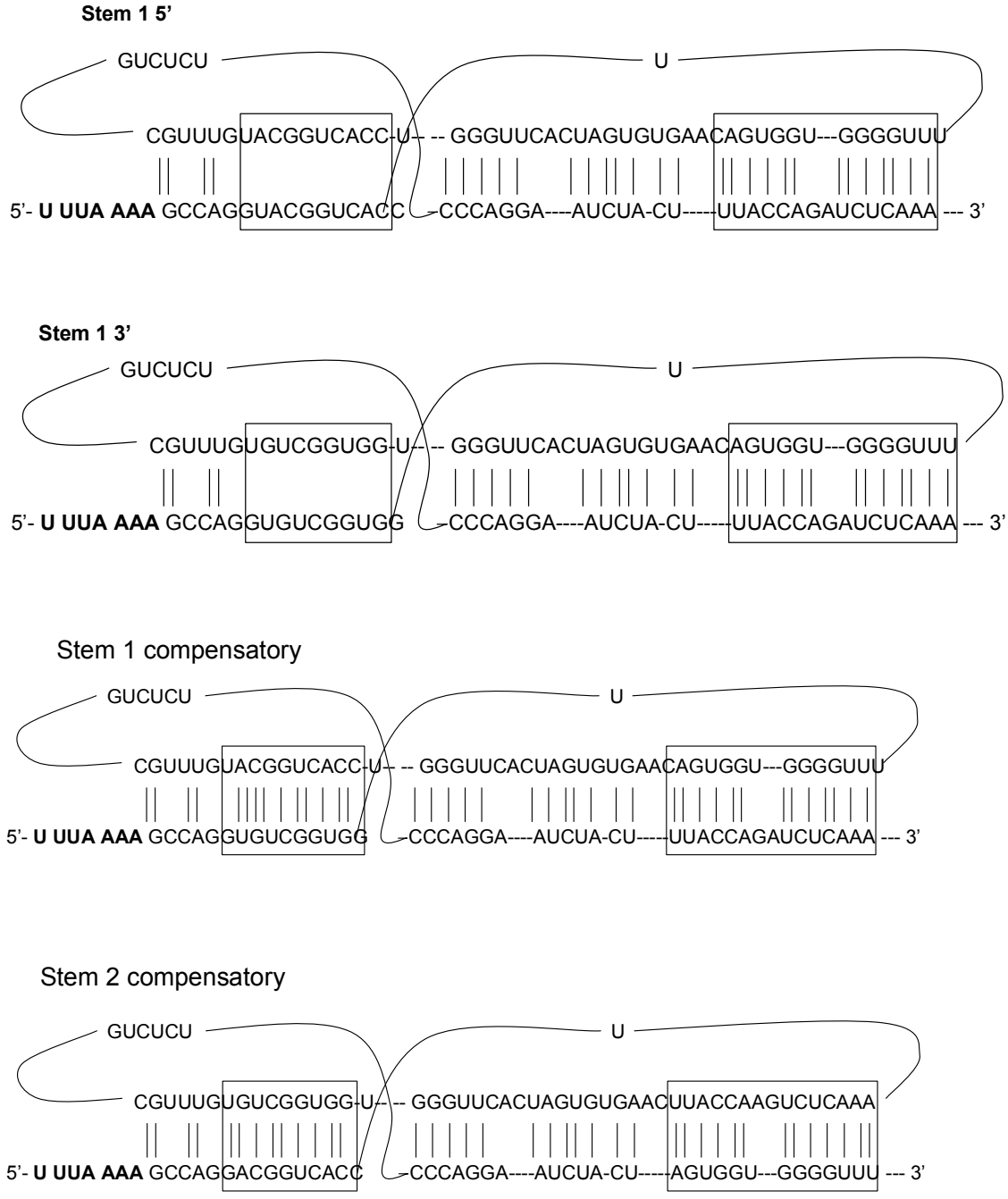

Figure 31. *Suggested further studies on the CCR5 frameshift signal*. Stem 1 and 2 are boxed, and the slippery site is in bold. Stem 1 is closer to the slippery site. Stem 1 should be disrupted and both stems should have compensatory mutations. Also, the structure of the CCR5 pseudoknot should be confirmed.

Furthermore, the structure of the CCR5 pseudoknot has only been predicted by computational mRNA folding programs. There is some secondary structure there because frameshifting occurs. However, the exact interactions are only predicted. The most likely structure as seen in Figure 23 is may not be the physiological structure. There is no spacer region, which is required so that the slippery site is positioned in the A and P sites of the ribosome. The lower part of stem 1 is likely unwound by the ribosome, similar to the HIV stem loop. The actual structure should be examined by structure probing and nuclease mapping.

The biological impact and significance of CCR5 frameshifting remains to be investigated. When CCR5 frameshifts, it produces a truncated protein product. The N-terminal 138 amino acids are the same in both the full length and truncated protein. The N-terminal is responsible for the binding to the HIV glycoprotein. It is not known whether the frameshift product is displayed on the cell surface or has any biological role.

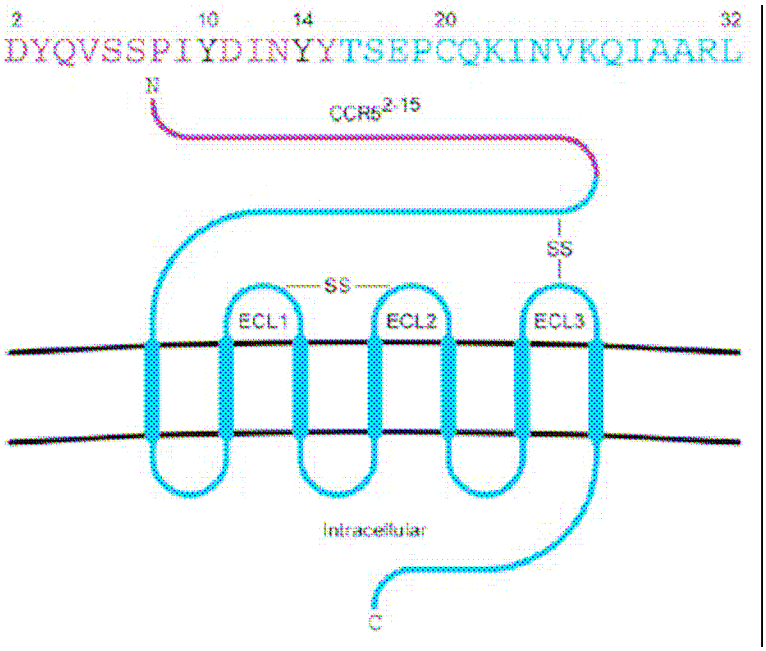

Figure 32. *Structure of CCR5 protein in the cell membrane*. Interaction with the HIV gp120 is with the N-terminal end and extracellular loop 2 (ECL2) (Huang *et al*, 2007). The 138 N-terminal amino acids are common in both the full length and truncated frameshift products.

If the frameshift product is indeed on the cell surface, it could be influential in HIV pathogenesis. Once CCR5 is bound by the HIV glycoprotein, HIV gp41 undergoes a conformational rearrangement and the membranes can fuse. Whether HIV could bind both CCR5 products or binds one preferentially over the other needs to be determined. This could be a potential target in treating HIV infections.

Bibliography

Amort, M., Wotzel, B., Bakowska-Zywicka, K., Erlacher, M.D., Micura, R., Polacek, N. (2007). An intact ribose moiety at A2602 of 23S rRNA is key to trigger peptidyl-tRNA hydrolysis during translation termination. Nucleic Acids Res. 2007;35(15):5130-40.

Andersen, C.B., Becker, T., Blau, M., Anand, M., Halic, M., Balar, B., Mielke, T., Boesen, T., Pedersen, J.S., Spahn, C.M., Kinzy, T.G., Andersen, G.R., and Beckmann, R. (2006). Structure of eEF3 and the mechanism of transfer RNA release from the E-site. Nature. 443(7112):663-8.

Baranov, P.V., Henderson, C.M., Anderson, C.B., Gesteland, R.F., Atkins, J.F., Howard, M.T. (2005). Programmed ribosomal frameshifting in decoding the SARS-CoV genome. Virology. 332(2):498-510.

Beringer, M. and Rodnina, M.V. (2007). The ribosomal peptidyl transferase. Mol Cell. 2007 May 11;26(3):311-21.

Berk, V., Zhang, W., Pai, R.D., and Cate, J.H. (2006). Structural basis for mRNA and tRNA positioning on the ribosome. Proc Natl Acad Sci. 103(43):15830-4.

Bieling, P., Beringer, M., Adio, S., and Rodnina, M.V. (2006). Peptide bond formation does not involve acid-base catalysis by ribosomal residues. Nat Struct Mol Biol. 13(5):423-8.

Brierley,I.A., Rolley,N.J., Jenner,A.J. and Inglis,S.C. (1991). Mutational analysis of the RNA pseudoknot component of a coronavirus ribosomal frameshifting signal. J. Mol. Biol., 220, 889–902.

Brierley, I. and Dos Ramos, F.J. (2006). Programmed ribosomal frameshifting in HIV-1 and the SARS-CoV. Virus Res. 119(1):29-42.

Cochella, L., Brunelle, J.L., and Green, R. (2007). Mutational analysis reveals two independent molecular requirements during transfer RNA selection on the ribosome. Nat Struct Mol Biol. 14(1):30-6.

Davidovich, C., Bashan, A., Auerbach-Nevo, T., Yaggie, R.D., Gontarek, R.R., Yonath, A. (2007). Induced-fit tightens pleuromutilins binding to ribosomes and remote interactions enable their selectivity. Proc Natl Acad Sci. Mar 13;104(11):4291-6.

Davies, J. and Davis, B.D. (1968). Misreading of ribonucleic acid code words induced by aminoglycoside antibiotics. *J. Biol. Chem.*, **243**, 3312–3316.

Demeshkina, N., Hirokawa, G., Kaji, A., and Kaji, H. (2007). Novel activity of eukaryotic translocase, eEF2: dissociation of the 80S ribosome into subunits with ATP but not with GTP. Nucleic Acids Res. 35(14):4597-607.

Dinman, J.D., Richter, S., Plant, E.P., Taylor, R.C., Hammell, A.B., and Rana, T.M. (2002). The frameshift signal of HIV-1 involves a potential intramolecular triplex RNA structure. Proc Natl Acad Sci. 99(8):5331-6.

Dinman, J.D. and Wickner, R.B. (1992). Ribosomal frameshifting efficiency and gag/gag-pol ratio are critical for yeast M1 double-stranded RNA virus propagation. J Virol. 1992 Jun;66(6):3669-76.

Dulude, D., Berchiche, Y.A., Gendron, K., Brakier-Gingras, L., Heveker, N. (2006). Decreasing the frameshift efficiency translates into an equivalent reduction of the replication of the human immunodeficiency virus type 1.Virology. Feb 5;345(1):127-36.

Ermolenko, D.N., Spiegel, P.C., Majumdar, Z.K., Hickerson, R.P., Clegg, R.M., and Noller, H.F. (2007). The antibiotic viomycin traps the ribosome in an intermediate state of translocation. Nat Struct Mol Biol. 14(6):493-7.

Fekete, C.A., Mitchell, S.F., Cherkasova, V.A., Applefield, D., Algire, M.A., Maag, D., Saini, A.K., Lorsch, J.R., and Hinnebusch, A.G. (2007). N- and C-terminal residues of eIF1A have opposing effects on the fidelity of start codon selection. EMBO J. 26(6):1602-14.

Giedroc, D.P., Theimer, C.A. and Nixon, P.L. (2000). Structure, stability and function of RNA pseudoknots involved in stimulating ribosomal frameshifting. J. Mol. Biol., 298, 167–185.

Gilbert, R.J., Gordiyenko, Y., von der Haar, T., Sonnen, A.F., Hofmann, G., Nardelli, M., Stuart, D.I., and McCarthy, J.E. (2007). Reconfiguration of yeast 40S ribosomal subunit domains by the translation initiation multifactor complex. Proc Natl Acad Sci. 104(14):5788-93.

Girnary, R., King, L., Robinson, L., Elston, R., and Brierley, I. (2007). Structure-function analysis of the ribosomal frameshifting signal of two human immunodeficiency virus type 1 isolates with increased resistance to viral protease inhibitors. J Gen Virol. 88(Pt 1):226-35.

Grentzmann, G., Ingram, J.A., Kelly, P.J., Gesteland, R.F., and Atkins, J.F. 1998. A dual-luciferase reporter system for studying recoding signals. *RNA* 4**:** 479–486.

Gualerzi, C., G. Risuleo, and C. L. Pon**.** 1977. Initial rate kinetic analysis of the mechanism of initiation complex formation and the role of initiation factor IF-3. Biochemistry 16**:**1684-1689.

Hansen, T.M., Reihani, S.N., Oddershede, L.B., Sorensen, M.A. (2007). Correlation between mechanical strength of messenger RNA pseudoknots and ribosomal frameshifting. Proc Natl Acad Sci. 104(14):5830-5.

Hirabayashi, N., Sato, N.S., and Suzuki, T. (2006). Conserved loop sequence of helix 69 in Escherichia coli 23 S rRNA is involved in A-site tRNA binding and translational fidelity. J Biol Chem. 281(25):17203-11.

Huang, C.C., Lam, S.N., Acharya, P., Tang, M., Xiang, S.H., Hussan, S.S., Stanfield, R.L., Robinson, J., Sodroski, J., Wilson, I.A., Wyatt, R., Bewley, C.A., Kwong, P.D. (2007). Structures of the CCR5 N terminus and of a tyrosine-sulfated antibody with HIV-1 gp120 and CD4. Science. Sep 28;317(5846):1930-4.

Jacks,T., Power,M.D., Masiarz,F.R., Luciw,PA., Barr,P.J., Varmus,H.E. (1988). Characterization of ribosomal frameshifting in HIV-1 gag-pol expression. Nature, 331, 280–283.

Jacobs, J.L. and Dinman, J.D. (2004). Systematic analysis of bicistronic reporter assay data. Nucleic Acids Res. 32(20):e160.

Kamitani, W., Narayanan, K., Huang, C., Lokugamage, K., Ikegami, T., Ito, N., Kubo, H., and Makino, S. (2006). Severe acute respiratory syndrome coronavirus nsp1 protein suppresses host gene expression by promoting host mRNA degradation. Proc Natl Acad Sci. 103(34):12885-90.

Karimi,R. and Ehrenberg,M. (1994). Dissociation rate of cognate peptidyl tRNA from the A-site of hyper-accurate and error-prone ribosomes. *Eur. J. Biochem.*, **226**, 355–360.

Konevega, A.L., Fischer, N., Semenkov, Y.P., Stark, H., Wintermeyer, W., and Rodnina, M.V. (2007) Spontaneous reverse movement of mRNA-bound tRNA through the ribosome. Nat Struct Mol Biol. 14(4):318-24.

Korostelev, A., Trakhanov, S., Laurberg, M., and Noller, H.F. (2006). Crystal structure of a 70S ribosome-tRNA complex reveals functional interactions and rearrangements. Cell. 126(6):1065-77.

Laursen, B.S., Sorensen, H.P., Mortensen, K.K., Sperling-Petersen, H.U. (2005). Initiation of protein synthesis in bacteria. Microbiol Mol Biol Rev. Mar;69(1):101-23.

Masters, P.S. (2006). The molecular biology of coronaviruses. Adv Virus Res. 66:193-292.

Munro, J.B., Altman, R.B., O'Connor, N., and Blanchard, S.C. (2007). Identification of two distinct hybrid state intermediates on the ribosome. Mol Cell. 25(4):505-17.

Namy, O., Moran, S.J., Stuart, D.I., Gilbert, R.J., and Brierley, I. (2006). A mechanical explanation of RNA pseudoknot function in programmed ribosomal frameshifting. Nature. 441(7090):244-7.

Nilsson J, Sengupta J, Gursky R, Nissen P, Frank J. (2007). Comparison of fungal 80S ribosomes by cryo-EM reveals diversity in structure and conformation of rRNA expansion segments. J Mol Biol. 369(2):429-438.

Ogle, J.M. and Ramakrishnan, V. (2005). Structural insights into translational fidelity. Annu Rev Biochem. 74:129-77.

Ogle, J.M., Carter, A.P., and Ramakrishnan, V. (2003). Insights into the decoding mechanism from recent ribosome structures. Trends Biochem Sci. 28(5):259-66.

Pan, D., Kirillov, S.V, and Cooperman, B.S. (2007). Kinetically competent intermediates in the translocation step of protein synthesis. Mol Cell. 25(4):519-29.

Plant, E. P., and Dinman, J. D. (2005). Torsional restraint: a new twist on frameshifting pseudoknots. Nucleic Acids Res *33*, 1825-1833.

Plant, E.P., and Dinman, J.D. (2006). Comparative study of the effects of heptameric slippery site composition on -1 frameshifting among different eukaryotic systems. RNA. 12(4):666-73.

Plant, E. P., Jacobs, K. L., Harger, J. W., Meskauskas, A., Jacobs, J. L., Baxter, J. L.,Petrov, A. N., and Dinman, J. D. (2003). The 9-A solution: how mRNA pseudoknots promote efficient programmed -1 ribosomal frameshifting. RNA *9*, 168-174.

Plant, E.P., Nguyen, P., Russ, J.R., Pittman, Y.R., Nguyen, T., Quesinberry, J.T., Kinzy, T.G., and Dinman, J.D. (2007). Differentiating between near- and non-cognate codons in Saccharomyces cerevisiae. PLoS ONE. 2(6):e517.

Plant, E. P., Perez-Alvarado, G. C., Jacobs, J. L., Mukhopadhyay, B., Hennig, M., and Dinman, J. D. (2005). A three-stemmed mRNA pseudoknot in the SARS coronavirus frameshift signal. PLoS Biol *3*, e172.

Plant, E. P., Wang, P., Jacobs, J. L., and Dinman, J. D. (2004). A programmed -1 ribosomal frameshift signal can function as a cis-acting mRNA destabilizing element. Nucleic Acids Res *32*, 784-790.

Polacek, N. and Mankin, A.S. (2005). The ribosomal peptidyl transferase center: structure, function, evolution, inhibition. Crit Rev Biochem Mol Biol. 2005 Sep-Oct; 40(5):285-311.

Puglisi,J.D., Wyatt,J.R. and Tinoco, I.,Jr (1988). A pseudoknotted RNA oligonucleotide. Nature, 331, 283–286.

Ramakrishnan, V. and White, S.W. (1998). Ribosomal protein structures: insights into the architecture, machinery and evolution of the ribosome. Trends Biochem Sci. 23(6):208-12.

Raman, A., Guarraia, C., Taliaferro, D., Stahl, G., and Farabaugh, P.J. (2006). An mRNA sequence derived from a programmed frameshifting signal decreases codon discrimination during translation initiation.RNA. 12(7):1154-60.

Rodnina, M.V., Beringer, M., Wintermeyer, W. (2007). How ribosomes make peptide bonds.Trends Biochem Sci. 2007 Jan;32(1):20-6.

Rodnina, M.V., Savelsbergh, A., and Wintermeyer, W. (1999). Dynamics of translation on the ribosome: molecular mechanics of translocation. FEMS Microbiol Rev. 23(3):317-33.

Rodnina, M.V. and Wintermeyer, W. (2003). Peptide bond formation on the ribosome: structure and mechanism. Curr Opin Struct Biol. 13(3):334-40.

Rota, P.A. *et al*. (2003). Characterization of a novel coronavirus associated with severe acute respiratory syndrome. Science. May 30;300(5624):1394-9.

Selmer, M., Dunham, C.M., Murphy, F.V. 4th, Weixlbaumer, A., Petry, S., Kelley, A.C., Weir, J.R., and Ramakrishnan, V. (2006). Structure of the 70S ribosome complexed with mRNA and tRNA. Science. 313(5795):1935-42.

Staple, D.W. and Butcher, S.E. (2005). Solution structure and thermodynamic investigation of the HIV-1 frameshift inducing element. J Mol Biol. Jun 24;349(5):1011-23.

Steinberg, S.V. and Boutorine, Y.I. (2007). G-ribo motif favors the formation of pseudoknots in ribosomal RNA. RNA. 13(7):1036-42.

Su, M.C., Chang, C.T., Chu, C.H., Tsai, C.H., and Chang, K.Y. (2005). An atypical RNA pseudoknot stimulator and an upstream attenuation signal for -1 ribosomal frameshifting of SARS coronavirus. Nucleic Acids Res. 33(13):4265-75.

Takyar,S., Hickerson,R.P. and Noller,H.F. (2005) mRNA helicase activity of the ribosome. Cell, 120, 49–58.

Taliaferro, D.L. and Farabaugh, P.J. (2007). Testing constraints on rRNA bases that make nonsequence-specific contacts with the codon-anticodon complex in the ribosomal A site. RNA *8*, 1279-86.

Taylor, D.J., Nilsson, J., Merrill, A.R., Andersen, G.R., Nissen, P, and Frank, J. (2007). Structures of modified eEF2 80S ribosome complexes reveal the role of GTP hydrolysis in translocation. EMBO J. 26(9):2421-31.

Thiel, V., Ivanov, K.A., Putics, A., Hertzig, T., Schelle, B., Bayer, S., Weissbrich, B., Snijder, E.J., Rabenau, H., Doerr, H.W., Gorbalenya, A.E., Ziebuhr, J. (2003). Mechanisms and enzymes involved in SARS coronavirus genome expression. J Gen Virol. 2003 Sep;84(Pt 9):2305-15.

Tu,C., Tzeng,T.-H. and Bruenn,J.A. (1992). Ribosomal movement impeded at a pseudoknot required for ribosomal frameshifting. Proc. Natl Acad. Sci. USA, 89, 8636–8640.

Uemura, S., Dorywalska, M., Lee, T.H., Kim, H.D., Puglisi, J.D., and Chu, S. (2007). Peptide bond formation destabilizes Shine-Dalgarno interaction on the ribosome. Nature. 446(7134):454-7.

Wang, X., Wong, S.M., and Liu, D.X. (2006). Identification of Hepta- and Octo-Uridine stretches as sole signals for programmed +1 and -1 ribosomal frameshifting during translation of SARS-CoV ORF 3a variants.Nucleic Acids Res. 34(4):1250-60.

Weiss, S.R. and Navas-Martin, S. (2005). Coronavirus pathogenesis and the emerging pathogen severe acute respiratory syndrome coronavirus. Microbiol Mol Biol Rev. 69(4):635-64.

Wills, N.M. and Atkins, J.F. (2006). The potential role of ribosomal frameshifting in generating aberrant proteins implicated in neurodegenerative diseases. RNA. 12(7):1149-53.

Wilson, D.N, and Nierhaus, K.H. (2003). The Ribosome through the Looking Glass. Angew. Chem. Int. Ed. *42*, 3464-3486.

Wilson, D.N, and Nierhaus, K.H. (2006). The E-site story: the importance of maintaining two tRNAs on the ribosome during protein synthesis. Cell Mol Life Sci. Dec;63(23):2725-37.

Yoshizawa, S., Fourmy, D., Puglisi, J.D. (1998). Structural origins of gentamicin antibiotic action. EMBO J. Nov 16;17(22):6437-48.

Yusupova, G., Jenner, L., Rees, B., Moras, D., and Yusupov, M. (2006). Structural basis for messenger RNA movement on the ribosome. Nature. 444(7117):391-4.